# Patient Setup Quality Assurance In External Beam Radiotherapy Using A Third-Party Treatment Setup Verification Software.

By

Mercy Torshie Schandorf

(10805141)

This thesis/dissertation is submitted to the University of Ghana, Legon, in partial fulfilment of the requirement for the award of MPhil Medical Physics degree.

December 2021

# DECLARATION

This thesis is the result of research work carried out by Mercy Torshie Schandorf in the Department of Medical Physics, School of Nuclear and Allied Sciences, University of Ghana, under the supervision of Mr Eric Addison, Dr Theresa Bebaaku Dery and Dr Afua Yorke. I hereby declare that no portion of this work has been submitted in whole or in part to any other university or institution for the purpose of conferring a diploma or degree at any level. As such, other authors' works and/or research cited in this work have been acknowledged in the references section.

Sign ..............................

Mercy Torshie Schandorf

(Student)

Date 15/12/2021

Sign..............................

Mr. Eric Addison

(Principal Supervisor)

Date 15/12/2021

Sign__________________

Dr. Theresa Bebaaku Dery

(Co-Supervisor)

Date 15/12/2021

Sign..............................

Dr. Afua Yorke

(Co-Supervisor)

Date 15/12/2021

# ABSTRACT

This study sought to assess the performance of a MATLAB algorithm (CORRO) as a quality assurance tool for the verification of treatment setup based on using megavoltage (MV) images from an Electronic Portal Imaging Device (EPID), and the treatment planning system's digitally reconstructed radiographs (DRRs) obtained from patients' three-dimensional (3D) computed tomography (CT) data sets. The individual treatment planning system's DRR was used as a reference radiograph to detect patient setup errors during radiotherapy treatment via the superimposition of the EPID Image on the DRR. Matching points on both images were placed on identical landmarks to facilitate the process. MV and kV (DRR) image pairs of thirty (30) anonymised patients who had received radiotherapy treatment on the Varian Medical System Clinac IX medical linear accelerator at the Komfo Anokye Teaching Hospital patients were employed in the study. Another Matlab algorithm (ASEMPA) was used to load the Anterior-Posterior (AP) and lateral (Lat) MV and kV image pairs for each patient at the same time, and the matching landmark spots on the image pairs were selected. The shifts' root mean square deviation was computed. The systematic error range for Prostate cases was determined to be 0.46 cm – 18.62 cm, while that for Head and Neck cases was found to be 1.57 cm – 11.56 cm. This revealed significant variances. These variables aided in calculating the setup variance and, as a result, the facility's setup accuracy.

# DEDICATION

I dedicate this work to my external family and siblings.

# ACKNOWLEDGEMENTS

Firstly, my gratitude firstly goes to God for seeing me through and to my supervisors, Dr Eric Addison, Dr Theresa Bebaaku Dery and Dr Afua Yorke, for the encouragement, constructive criticism, guidance and for all the support given me throughout my dissertation.

Additionally, I would like to express my gratitude to the staff of the Medical Physics Department at the School of Nuclear and Allied Sciences for providing me with the opportunity to conduct this study and for all of the contributions made during the various presentations.

I am grateful to the entire Medical Physics Department staff at Komfo Anokye Teaching Hospital for their hospitality, availability and support throughout my stay at the facility during my data collection.

Last but not the least, to my entire family and my supportive friends, I was truly blessed to have you as my support system during this endeavour. Thank you for always being there, even in times when I did not notice I needed support.

# TABLE OF CONTENTS

LIST OF FIGURES

# LIST OF TABLES

# ABBREVIATIONS

2D – Two Dimensional

3D- Three Dimensional

AP- Anterior – Posterior

ASEMPA – Assisted Expert Manual Point Selection Application

cm - centimetre

CT - Computed Tomography

CORRO - Combinatorial Rigid Registration Optimization

DICOM – Digital Imaging and Communications in Medicine.

DIR - Deformable Image Registration

DRR – Digitally Reconstructed Radiographs

EBRT - External Beam Radiation Therapy

EPI- Electronic Portal Images

EPID – Electronic Portal Imaging Device

IGRT - Image-Guided Radiation Therapy

IMRT- Intensity-Modulated Radiation Therapy

IRB – Institutional Review Board

KATH - Komfo Anokye Teaching Hospital

kV – Kilo Voltage

Lat – Lateral

LDR – Low Dose Rate

LINAC- Linear Accelerator

MLC – Multileaf Collimator

mm- Millimetre

MRI – Magnetic Resonance Imaging

MV – Mega Voltage

NAL – No Action Level

OPD - Outpatient Department

SAL – Shrinking Action Level

TPS – Treatment Planning System

QA – Quality Assurance

# CHAPTER ONE

## INTRODUCTION

### 1.1 BACKGROUND OF THE STUDY

The main goal of radiotherapy is the delivery of an optimal dose to the targeted volume while minimising the dose to adjacent normal tissues (Kron, 2008). External Beam Radiation Therapy (EBRT) typically accomplishes this goal by employing multiple beams to ensure an even distribution of doses within the volume targeted and to minimise normal tissue complications. Different gantry angles are used for these multiple beams. External beam radiotherapy techniques require positioning and the use of immobilisation devices to ensure accurate tumour localisation and treatment setup reproducibility. Patients lie on a treatment couch in prone or supine anatomical positions during treatment deliveries, depending on the location of the target volume. Accurate and reproducible patient setup using Image Guided Radiation Therapy (IGRT) requires registering the daily treatment images to the reference planning CT image set (Verellen, 2008). Imaging advances have revolutionised the delineation of target volume and organs at risk for radiation oncology treatment planning. To confirm patient positioning, digitally reconstructed radiographs (DRR) from a treatment plan system are usually compared to portal images obtained with a treatment machine in either analog (radiograph) or digital format. The digital formats are communicated and managed using Digital Imaging and Communications in Medicine (DICOM). DICOM is the de facto standard in the industry for an image file format for radiological hardware (Graham et al., 2005). For proper utilisation, consistent portal image quality and a stable radiation response are required, which necessitates routine quality assurance (QA). In contemporary radiation therapy, digitally reconstructed radiographs are critical. They are planar x-rays generated using the same axial computed tomography (CT) data sets as those used for the treatment planning that is taken with the patient in the treatment position according to a specific coordinate system. There are three coordinate systems: patient coordinate system, coordinate room system, and beam coordinate system. These systems must be factored in when planning patient treatment to avoid misorientation because they differ. Therefore, transforming different data sets into a coordinate system is necessary to compare or integrate the data obtained from these different measurements (image registration). There are four widely used techniques for evaluating the integrity of image registration: visual inspection, fiducials, landmark point sets, and mutual information. (Yorke et al., 2020). The patient position deviation can be calculated using the landmark point method to assess the images. Before beam delivery, the correction is used to align the patient nearly perfectly with the reference image position.

## 1.2 STATEMENT OF RESEARCH PROBLEM

Radiation therapy is the most frequently used modality for cancer management, necessitating ongoing research and development of procedures that ensure dose sparing of critical structures and accurate dose to treatment volumes due to the fact that its effect cannot be reversed. Additionally, when new accessories are used, an in-depth examination of their effect on the relevant beam parameters are required. The following were identified for this study:

The portal imaging device used at the study facility placed a higher premium on quality assurance (QA) of significant errors in treatment ports or setup, with a lower priority on daily image guidance for more precise treatment delivery. Over the years, physicians visually verified registered images by comparing portal and diagnostic quality images to a digitally reconstructed radiograph (DRR). The accuracy with which this method of evaluating the quality of image registration is applied has been reported to be between 5 to 10 mm (Clippe et al., 2003). However, this method of registration is subjective and therefore unsuitable for large amounts of data.

Currently, Komfo Anokye Teaching Hospital (KATH) uses visual inspection, fiducial, and landmark point methods to verify the patient's alignment, and these methods are subjective. The facility does not have the means to quantify the deviation occurring in the setup. Therefore, there is a need to input a system that will quantify the deviations for optimal patient alignment and reduce the unevaluated incidences of exposure to healthy tissues. The problem is to evaluate the suitability of the combinatorial rigid registration optimisation (CORRO) algorithm to give the optimal patient setup and optimise patient setup reproducibility at KATH. Figure 1 shows the setup of the treatment offline review of a patient. Figure 2 shows the setup verification image of a patient.

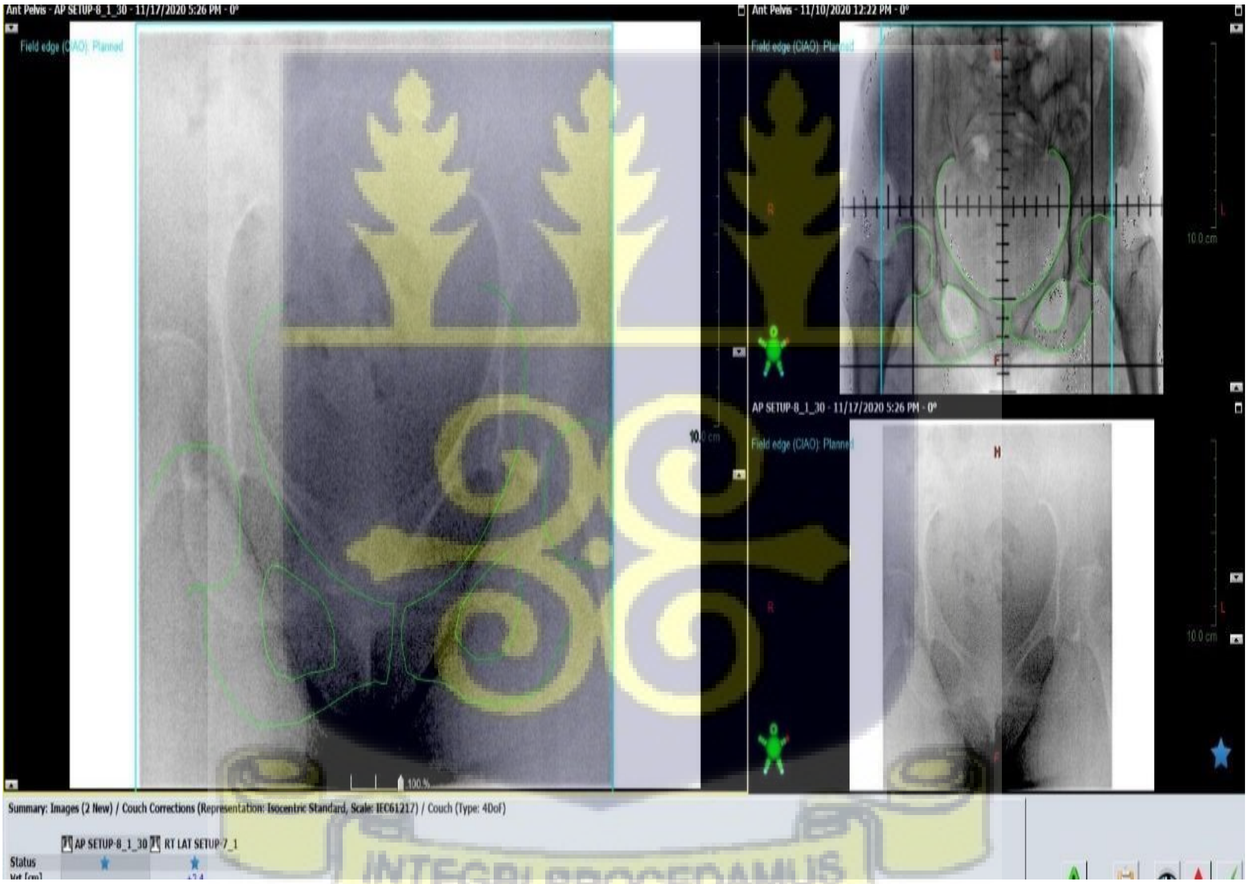

Figure 1: A Treatment Offline Review of Patient Setup from the LINAC Machine

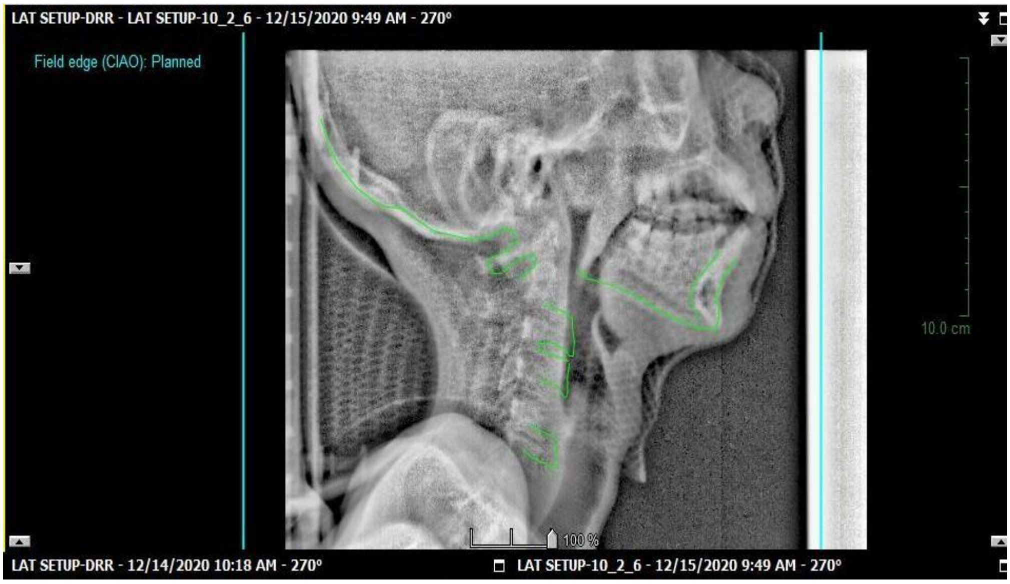


Figure 2: A Patient Setup Verification Image

## 1.3 OBJECTIVES OF THE STUDY

The overall aim of this study is to demonstrate the suitability of using combinatorial rigid registration optimisation (CORRO) to determine the optimal alignment of clinical image pairs for rigid registration at Komfo Anokye Teaching Hospital (KATH).

This specifically led to the following:

1. To perform patient-specific quality assurance on radiotherapy setup and determine output registration deviations.
2. To evaluate the accuracy of patient positioning in the facility.

## 1.4 SIGNIFICANCE AND JUSTIFICATION OF THE STUDY

Clinical image pairings provide the most accurate test data for evaluating image registration. This assists in making sure that minimum healthy tissues are being irradiated. These images allow for the evaluation of the treatment isocenter and field edges in relation to the patient's position. This research study will assess the suitability of CORRO for assessing the patient positioning into near-perfect alignment with the aid of reference images (DRR) and verification images (MV images).

It also seeks to probe into the accuracy of the patient setup reproducibility at KATH and analyse the deviation in setup during treatment.

## 1.5 SCOPE OF THE STUDY AND LIMITATIONS

The study analysed DRR image data from a CT scanner and verification images taken during treatment with an EPID for thirty (30) cases involving the head and neck and pelvic anatomic regions at the Komfo Anokye Teaching Hospital, Oncology Department, where patient setup using MV portal imaging and a digitally reconstructed radiograph is currently used for radiotherapy treatment verification.

Some limitations experienced during this work were the poor contrast in the verification images (MV images), versions of MATLAB not being able to support the code used in the work, resizing of the images to be of the same size proved to be a difficult, delay in getting ethical clearance and finally difficulty in resizing the DRR images.

## 1.6 ORGANISATION OF THE STUDY

The study is divided into five chapters. Chapter one introduces the research by summarising the study's relevance and justification. Additionally, it describes the problem being addressed and the objectives for resolving it. This chapter also discusses the study's scope and limitations.

The second chapter summarises the literature pertinent to the research problem. The third chapter discusses the research materials and methods used to conduct the study. The experimental procedure for ensuring the quality of patient setup is described using the MV portal imaging, and digitally reconstructed radiograph radiotherapy practices are also discussed. The experimental results and discussion were presented in Chapter four. Finally, chapter five summarises the findings, makes recommendations, and makes suggestions for future research.

# CHAPTER TWO

## LITERATURE REVIEW

### 2.1 RADIOTHERAPY

Radiotherapy incorporates imaging data into treatment planning and delivery, even more so when the target is not superficial. Regardless of the treatment circumstances, there will always be considerable uncertainty in precisely defining the target position during dose delivery in a given fraction or between successive fractions. A straightforward strategy for increasing overall treatment accuracy is to minimise systematic deviations in the patient setup by implementing a setup verification protocol during treatment (Pehlivan et al., 2009).

External beam radiotherapy is a technique in which high-energy beams are directed from a distance toward the patient's tumour. Typically, these beams are generated externally to the patient's body using linear accelerators or teletherapy cobalt-60 units. A linear accelerator for medical applications (LINAC) uses high-energy x-rays or electrons to irradiate the tumour volume; destroying cancer cells while sparing normal tissue in the surrounding area. The linear accelerator uses microwave technology (similar to that used in radar) to accelerate electrons in a section of the accelerator called the "waveguide," allowing these electrons to collide with a heavy metal target and generate high-energy x-rays. When these high-energy x-rays exit the machine, they are shaped to match the shape of the patient's tumour, and the resulting individualised beam is directed at the tumour. Typically, a multileaf collimator integrated into the machine's head shapes the beam. The patient is positioned on a movable treatment couch and lasers are used to monitor the patient's alignment. The therapy couch can be adjusted in a variety of directions, including motions in the vertical, lateral and horizontal planes. The beam exits the accelerator through a rotating section known as a gantry. Radiation can be delivered to the tumour from a variety of angles by rotating the gantry and repositioning the treatment couch.

Numerous safety features ensure that the prescribed dose is delivered correctly, and it is routinely inspected for proper operation by a medical physicist. Radiation therapy can be used in conjunction with other cancer treatment modalities, such as surgery or chemotherapy. It is used either preoperatively to shrink the tumour and make it more accessible for removal or postoperatively to eradicate those that have invaded lymph nodes, blood vessels, and other tissues. External Beam Radiation Treatment (EBRT) can be used to treat conditions on a palliative or curative basis. Patients are typically treated once daily in the outpatient department (OPD) for approximately two to nine weeks, depending on the patient's diagnosis and delivery modality, such as intensity-modulated radiation (IMRT). For LINAC-based radiation therapy, the radiation oncologist collaborates with a radiation dosimetrist and a medical physicist to customize the treatment plan. Prior to initiating treatment, they will validate this plan and implement quality control measures to ensure that each treatment is administered consistently.

## 2.2 IMAGE-GUIDED RADIOTHERAPY

Image-guided radiation therapy (IGRT) is a type of radiation therapy in which each treatment session incorporates imaging techniques. IGRT combines imaging and therapy to improve the precision and accuracy of the target localization and treatment efficacy. While Intensity Modulated Radiation Therapy (IMRT) also uses imaging for target localization, it also employs cutting-edge software and sophisticated hardware to precisely control the intensity and shape of radiation delivered to various treatment areas. By incorporating detailed images, IGRT ensures that the high-intensity radiation is focused precisely on the treatment area. When someone is treated with IGRT, high-quality images are taken prior to each radiation therapy session. As a result, IGRT may enable higher radiation doses to be used, increasing the likelihood of tumour control and typically resulting in shorter treatment schedules. IGRT is considered to be the standard of radiation therapy treatment. It is used to treat cancers of all types. Additionally, IGRT is beneficial for tumours that are prone to move during or between treatments. It is incorporated into radiation treatment plans because it enables more precise radiation delivery, improved definition, localisation, and monitoring of tumor position, size, and shape prior to and during treatment, the possibility of increasing the targeted radiation dose to achieve better tumour control, and decreased radiation exposure to normal tissue surrounding the tumour.

Image-guided radiation therapy in KATH is done when digitally reconstructed radiographs (DRR) generated from simulation CT images are matched (3D -2D) with MV electronic portal images. The portal images taken before treatment is achieved with either a kV or an MV onboard imager. In the case of KATH, the MV onboard imager is used

### 2.2.1 Digitally Reconstructed Radiographs

A digitally reconstructed radiograph (DRR), which is used to verify treatment in CT simulation, is one of the critical images that can be transmitted via radiotherapy communication (Hashimoto,2001). DRR images are created by digitally reconstructing an image created by a Three-Dimensional (3D) imaging system such as a Computed Tomography (CT) scan or Magnetic Resonance Imaging (MRI) in order to create a new Two-Dimensional (2D) Image that resembles a medical X-ray scan. They are usually used alongside a portal image to assist in patient setup. They, therefore, play a very significant role in the reproducibility of patient positioning and virtual simulation. In comparison to conventional radiography and computed radiography, digitally reconstructed radiographs can produce higher-quality images with lower X-ray exposures. The contrast is primarily affected by the average photon energy used to generate the Image, which is determined by the x-ray tube voltage used and the amount of x-ray beam filtration used; with decreasing photon energy, the differential attenuation between the lesion and the surrounding tissues increases. The cost of replacing existing radiographic equipment is probably the greatest disadvantage of digital radiography.

### 2.2.2 Electronic Portal Imaging Device

An electronic portal imaging device (EPID) enables the visualisation of a patient's anatomy while only administering a small fraction of the total radiation dose. After acquiring the electronic portal Image (EPI) and before continuing with the full dose delivery, a comparison of the patient's EPI to a reference image must be extremely fast and precise if positioning errors are to be evaluated with the intent of repositioning the patient, if necessary, before completing the treatment. Visual inspections alone may be used to conduct the comparison. However, visual inspection alone does not provide the quantitative accuracy required to align anatomy to within about 5 mm (Dong & Boyer, 1995). The use of EPIDs (electronic portal imaging devices) may provide a more efficient but far from "cost-free" method, which is contingent upon improvements in data acquisition speed and spatial resolution (LoSasso et al., 2001).


Figure 3: An Image of an Electronic Portal Imaging Device.

## 2.3 QUALITY ASSURANCE

Quality assurance in radiotherapy refers to all procedures that ensure the consistency of the medical prescription and its safe execution in terms of dose to the target volume, as well as minimal dose to normal tissue, minimal personnel exposure, and adequate patient monitoring.

Radiation therapy errors are defined as any deviation or shift from the intended or planned course of treatment. These errors may be the result of a mechanical issue or patient setup uncertainty. These include treatment parameters such as couch and gantry motions, as well as the patient's ability to maintain a comfortable position throughout the duration of the treatment (Herk, 2004). Uncertainties in fractionation can be caused by systematic or random errors. If errors in patient positioning, simulation, or target delineation are not corrected, they will affect all treatment fractions uniformly. This is known as a systematic error.

Random, on the other hand, is unpredictably variable with each fraction. Clinical margins are added to the clinical tumour volume to accommodate for errors (Stroom and Heijmen, 2008). When conformal treatment fields with a tight tumour margin are used, minimal deviation in patient setup on the treatment machine ensures maximum dose delivery to tumour cells while limiting dose to surrounding healthy tissues; thus, demand necessitates a higher level or degree of accuracy. In a sense, tight margins limit the degree of uncertainty (Lebsesque et al., 1992)

The linear accelerator's quality assurance is critical. Numerous systems are integrated into the accelerator to prevent it from exceeding the dose prescribed by the radiation oncologist. Each morning, prior to treating a patient, the medical physicist checks the machine to ensure that the radiation intensity is consistent across the beam and it is operating properly. Additionally, the medical physicist inspects the linear accelerator more thoroughly on a monthly and annual basis.

## 2.4 PATIENT SIMULATION

A clinical patient, before undergoing treatment, may either undergo conventional simulation or CT simulation, depending on the stage of cancer. Simulation is a way to mimic normal treatment procedures and find the best patient setup positioning for treatment. In its sense, simulation ensures a high degree of reproducibility during the entire treatment duration. Positioning and immobilisation devices are used to position and secure patients, as well as permanent marks and tattoos, to obtain images of the treatment area during simulation. These marks, tattoos, and devices serve as an alignment guide for patients as they begin daily treatment. After acquiring the images, they are loaded into a treatment planning system. Finally, the radiation dose delivered to the tumour and adjacent tissue is calculated using a specialised computer programme.

To achieve an effective treatment outcome, a treatment plan must be developed that delivers the appropriate dose to the tumour while sparing or minimising the dose to normal tissues. Treatment delivery techniques have been developed over the years, and these techniques have evolved in a series of stages. By determining the minimum objective function that best represents the alignment quality, the registration process geometrically aligns two images (typically, the mean squared error is a rigid registration transformation matrix). However, due to the lack of underlying ground truth, validating and quantifying the quality of the image registration remains a difficult problem in clinical practice.

## 2.5 IMAGE REGISTRATION

Visual inspection, fiducials, landmark point sets, and mutual information are the four most frequently used methods for evaluating the quality of registrations. Historically, physicians have verified registered images visually by examining portal and diagnostic quality images, as well as a planning digital reconstructed radiograph (DRR). An in-field metric (graticule attached to the MV treatment head) for detecting shared anatomical components between the portal Image and DRR. Bony anatomy is frequently used to evaluate the quality of image registration. The accuracy of the method is estimated to be between 5 and 10 millimetres (Clippe et al, 2003). However, this method of data registration is subjective and ineffective when dealing with large amounts of data.

A rigid image registration's ground truth has also been established using fiducial markers on phantoms and patients. Gold markers implanted in the prostate enhance prostate targeting for surgical procedures and radiotherapy treatment, as well as estimating registration error in kV or MV x-ray imaging. While fiducials remain attached to the target anatomy, they have been observed to drift away from their original fixed location due to changes in the target anatomy overtime or due to fiducial detachment. The interobserver error could occur as a result of the effect of fiducial relocation on registration. Additionally, the number of fiducials that can be fixed simultaneously is limited. O'Neill et al., 2016, discovered that approximately 66% of their patients had intrafraction motion greater than 2 millimeters in a study of 427 patients undergoing intensity-modulated radiation therapy with fiducial marker IGRT. Additionally, expert-positioned landmark point pairs were used to quantitatively validate the registration. These landmark points serve as the ground truth for linked images, allowing for confirmation based on the accuracy of the manually or automatically selected points.

### 2.5.1 Methods of Image Registration

There are several methods used for image registration, but there are four commonly used methods in patient setup. These methods include visual inspection for patient setup, the use of fiducials, the landmark method, and the use of mutual information.

2.5.1.1 Visual Inspection

Traditionally, treatment setup verification is accomplished through a qualitative visual comparison of portal films to simulation films or to each other. This method is subjective and cannot be completely relied on as it is dependent on the individual verifying the alignment's impression of a perfect alignment. Visual inspection is inexact, time-consuming, and is typically performed only once a week, at most, in numerous radiation oncology departments to ensure proper patient setup (Clippe et al., 2003)). This evaluating method of the registration quality typically involves the use of an in-field metric (graticule mounted to the MV treatment head) to identify shared anatomical structures between the portal and DRR images, most commonly the bony anatomy. This method has been reported to be accurate to within a range of 5 and 10 mm (Clippe et al., 2003). Due to the subjective nature of this method of registration, it is unsuitable for large amounts of data.

2.5.1.2 Use of Fiducials

Radio markers such as gold markers are used in this method to verify patient positioning. Fiducial markers placed on phantoms and patients were used to establish the ground truth for rigid image registration. Due to the visibility of gold markers implanted in the prostate during kV or MV x-ray imaging, they are used to improve prostate surgery and radiotherapy targeting (external beam radiotherapy), as well as to estimate registration error. The efficacy of this method is contingent upon the fixation of the fiducial markers in the prostate, the absence of significant prostate deformations during treatment, and the precision with which the marker position can be measured. Offline correction protocols such as the shrinking-action-level (SAL) and no-action-level (NAL) are frequently used to reduce the average position deviation during treatment. While the fiducials are fixed to the target anatomy, they are known to drift away from the original fixed point due to changes in the target anatomy over time or due to the fiducial detaching. The effect of fiducial relocation on the registration process may result in an interobserver error. Additionally, the total number of fiducials that can be fixed at any point in time is restricted (Poggi et al., 2003)

#### 2.5.1.3 Landmark Point Sets

Expert landmark correspondences are frequently used to assess the spatial accuracy of deformable image registration (DIR). Clinical studies have demonstrated that surface-matching techniques utilising laser scanners are more involved than point-matching techniques. They have numerous issues with robustness and exhibit a loss of accuracy when images are scanned and registered with different facial expressions. In point-matching registration, which is the most frequently used technique in practice, a set of at least three linearly independent positions in both the verification and reference images should be identified. A spatial transformation is computed that rigidly rotates and transcribes the corresponding points between two spaces until accurate alignment between the corresponding points is achieved (Kim et al., 2001). This method has proved to be a quantitative method that can be used in determining the disparities occurring in patient setup. This method was used in the study.

#### 2.5.1.4 Mutual Information

Mutual information-based registration has become widely used in a variety of clinical applications. Numerous papers describe the method as a component of a larger technique or application. Wood et al.1992, introduced the concept of using a registration measure for multimodality images, assuming that regions of similar tissue (and thus, similar grey values) in one Image correspond to regions of similar grey values in the other Image (though probably different values to those of the first Image). In an ideal world, the ratio of grey values for all corresponding points within a given region of either Image should be relatively constant. As a result, the average variance of this ratio is kept as low as possible across all regions to ensure registration.

## 2.6 PATIENT POSITIONING

External radiation therapy has as one of its goals the replication of the patient's position during each fraction of the treatment process. Two distinct types of patient setup correction strategies have been proposed in various types of literature: online and offline setup corrections. Before the actual treatment is administered, online correction of the patient setup position will assist in correcting for both systematic and random deviations (Aaner et al., 2005). There are several parameters that are put in place to aid in the reproducibility of the patient setup. Some of these are the use of room lasers, the use of fiducials, tattoos, field lights, the use of head and neck masks and the taking of verification images before treatment.

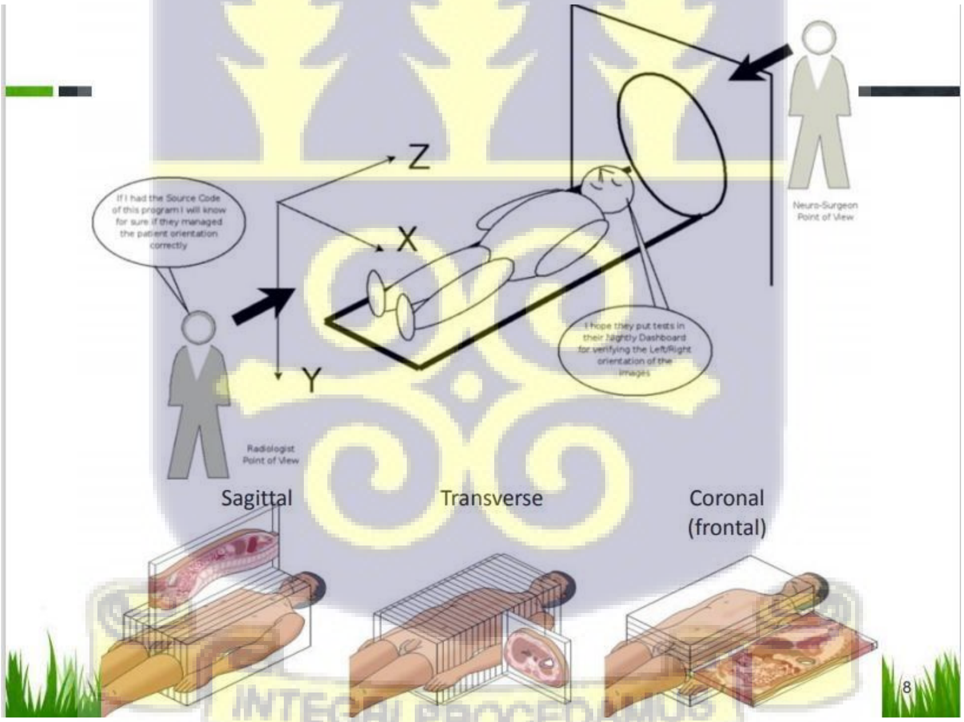


Source**:** http://mrl.cs.uh.edu/FMI_Fall_2013.html

Figure 4:. Patient Positioning Views and Sectioning

## 2.7 DIGITAL IMAGING AND COMMUNICATIONS IN MEDICINE (DICOM)

DICOM is the international standard for communicating and managing medical imaging data and associated information. Its mission is to ensure interoperability between systems that create, store, share, display, transmit, query, process, retrieval and printing of medical images, as well as associated workflow management.

DICOM is a compressed image format similar to the jpg format used to capture and save standard photographs. Physicians can view medical images in the DICOM format using a webbased image viewer. The resulting images are compressed and archived in the DICOM format, which significantly simplifies storage and retrieval compared to traditional x-ray films. The images are captured using high-resolution diagnostic cameras and are used in a variety of diagnostic procedures, ranging from diagnostic endoscopy to standard medical x-ray scanning.

DICOM technology has a number of advantages, one of which is that it takes seconds to "develop" the Image, as opposed to several hours for x-ray films. Increased speed benefits patients by improving their care, as well as workflow and healthcare efficiency. The second advantage of DICOM imaging is that physicians and other caregivers can access the images from any workstation located throughout the hospital or care facility.

DICOMs have two drawbacks: their large file sizes and the requirement for special software to view them on personal computers. Outside of radiology departments, the majority of personal computers are equipped with the Windows® operating system, which is incompatible with the DICOM file format. Thus, in order to incorporate DICOM images into PowerPoint® presentations, create teaching files, or publish Web pages, they must first be converted to Windows®-compatible image formats.

## 2.8 MATLAB SOFTWARE

MATLAB is a proprietary multi-paradigm programming language and a mathematical computing environment developed by MathWorks. MATLAB facilitates matrix manipulation, function and data visualisation, algorithm implementation, user interface design, and interfacing with programs written in other languages.

It allows a user to easily implement and test his/her algorithms, easily create computational codes, easily debug them, and utilise a large database of pre-configured algorithms. It's simple to process still images and create simulation videos. It also makes use of external libraries, conducts indepth data analysis and visualisation, and, last but not least, creates applications with a graphical user interface (MATLAB Resources, 2021).

Regardless of the many benefits MATLAB has, it is an interpreted language; hence it takes a little more time to execute as compared to other programming languages. It is costly and requires a powerful computer with sufficient memory. This study made use of the MATLAB software as shown in Appendix A.

## 2.9 ASSISTED EXPERT MANUAL POINT SELECTION APPLICATION (ASEMPA) AND COMBINATORIAL RIGID REGISTRATION OPTIMIZATION (CORRO)

Assisted Expert Manual Point selection Application is an interface that aids an expert to manually select landmark points on image pairs This application loads image pairs into a MATLAB algorithm and allows the user to pick mutual points on either corners, angles or the image pairs which is then run through another algorithm called the Combinatorial Rigid Registration Optimization to provides the image registration on the image pairs as shown in Appendix B.

# CHAPTER THREE

## MATERIALS AND METHODOLOGY

### 3.1 LIST OF MATERIALS / EQUIPMENT

The following materials and equipment: a Clinac IX linear accelerator, the Siemens CT Scanner, the Eclipse Treatment Planning System, the CORRO algorithm, and the Microsoft Excel and MATLAB software were used in this study.

#### 3.1.1 Computerised Tomography Scanner

The Computerised Tomography (CT) scanner used in this study is a Siemens 16 slice Somatom Emotion (Siemens AG, Wittelsbacherplatz 2, DE-90333 Muenchen, Germany). It features a 16-detector configuration with a 0.8x0.5 mm focal spot that enables 16x1.2 mm multislice imaging. It is identified by model number 10165880 and serial number 40438. CareDose4D is used to provide automatic exposure control. This enables automatic adjustment of the tube current in all three dimensions (x, y, and z-axis) to maintain constant image quality regardless of the size and area scanned. X-ray tube potentials attainable on the scanner are: 80 kV, 110 kV, and 130 kV.

Figure 5: An Image of the Siemen's 16 slices Somatom Emotion used for the study

### 3.1.2 Varian Linear Accelerator Clinac IX

The Varian Clinac IX linear accelerator was installed at the Oncology Directorate of the Komfo Anokye Teaching Hospital in 2017 and it is used for 2D and 3D conformal external beam energies. The Clinac IX is designed to generate a therapeutic beam of high-energy electrons or photons. It is capable of producing dual-energy photon beams (6 MV and 16 MV) and four electron beam energies (6MeV, 9MeV, 12MeV and 16MeV). It features a unique multileaf collimator (MLC) system with leaves for conformal radiation field shaping.


Figure 6: An Image of the Varian Clinac IX used at KATH

### 3.1.3 Eclipse Treatment Planning System

Treatment Planning with a computerised treatment planning system is the process of using a specialised computer to simulate the treatment delivery process for a patient to realise beam irradiation geometries and dose distributions within the irradiated volume. This helps clinicians to forecast the outcomes of treatment. The treatment planning system (TPS) uses mathematical algorithms that can be used to predict the physics of the interaction mechanism of the radiation and the traversing medium to estimate the dose distributions within a patient based on certain beam data acquired in a water phantom. The TPS in use at the study site is the Eclipse treatment planning system from Varian Medical System, Palo Alto, USA, and utilises the Analytical Anisotropic Algorithm (AAA) for dose calculation. The version of the Eclipse TPS is version 15.9.

Firstly, the treatment planning process would require a model of a patient to be treated to be generated from the axial CT data set of the patient in the treatment position. The axial CT data set is also used to create DRRs using the TPS's virtual treatment machine, similar to one to be used to treat the patient. The TPS is linked to a server and achieving system such that treatment parameters and DRRs to facilitate the verification of a patient setup for a finalised plan can be transferred and stored. The ARIA record and verifying system are used to ensure effective communication and smooth flow of information between the TPS and the achieving system. The treatment machine is also linked to this local area network to facilitate the automatic transfer of treatment parameters to the linear accelerator. The Eclipse TPS uses the Windows 7 operating system (Microsoft, USA) and features an intuitive user interface; as a result, users can quickly generate treatment plans to estimate expected dose distributions during the proposed treatment.

### 3.1.4 Combinatorial Rigid Registration Optimisation (Corro) Algorithm

CORRO, an in-house MATLAB-based algorithm, calculates the rigid registration using landmark points. These landmark points are manually selected between images by an expert using an in-house developed MATLAB interface called ASEMPA. Once the landmarks for an image set have been collected, a k-combination set is generated. A k-combination set is created as a subset of the landmark set by combining k consecutive pairs of landmarks. It estimates the k-mean of the rigid registration and its associated error after generating a large set of k combination sets for each case. The k-mean is calculated by averaging all the translations output by the k-set registration and subtracting the standard deviation (registration error). The results are validated by examining the central limit theorem of the rigid-k-mean registrations and their associated error. The k-mean is calculated by averaging all translations provided by the k-set registration outputs and subtracting the standard deviation from the mean (registration error). The central limit theorem is used to determine if the sample size is large (Yorke et al., 2020)

### 3.1.5 Study Site

The study site was the Radiotheraphy Department at the Oncology Directorate of Komfo Anokye Teaching Hospital (KATH). It is located in Kumasi, Ashanti Region, Ghana, is the second-largest hospital in Ghana, and the only tertiary health institution in the Ashanti Region (Govindaraj et al., 2022). The KATH Oncology Directorate provides outpatient services: radiation oncology, medical oncology, and haematology. The directorate provides several services and procedures such as, consultation, bone marrow aspiration, fine needle aspiration, chemotherapy, brachytherapy, teletherapy, simulation, radiotherapy planning, blood transfusion, tapping of ascitic fluid, injection, block moulding and formation of mask (KATH, 2022).

The Oncology Directorate is resourced with a medical linear accelerator, cobalt 60 teletherapy unit, X ray simulator, Low Dose Rate (LDR) brachytherapy, and 3D and 2D treatment planning systems to provide cancer care to patients in areas ranging from primary, secondary and tertiary care. Quality Control and Quality Assurance are done on the various machines at the department to make sure the machines give their utmost best when delivering services. The centre treats all cancers, with over 1200 patients treated yearly.

## 3.2 METHOD

### 3.2.1 Ethical Consideration

The sensitivity of the data to be used and patients' privacy, ethical clearance was sought from both the University of Ghana Ethical Committee for Basic and Applied Sciences and the Komfo Anokye Teaching Hospital's IRB as shown in Appendix C and D.

### 3.2.2 Ethical Issues

There was no danger of causing injury to the patients in this research because the images taken were not linked with their real identities, and physical contact with the patients was avoided. There were no known dangers associated with involvement that exceeded those faced in daily life. The advantages of employing CORRO software to determine positioning include its accuracy and its serving as a secondary check to quantify setup deviations which currently is lacking in the existing approach at the facility.



### 3.2.3 Confidentiality

Due to the absence of actual patients in this investigation, no vulnerable volunteers were considered. This study did not require participants to complete a permission form. However, because the report was based on DRR and verification images of treated patients, their names were not published. Confidential and anonymous patient information was maintained. The image pairs of the patients were duplicated and coded. Patients whose image pairs were used did not have their names published in the thesis or would in any future publication, and no information disclosed would be used against them in the future.

### 3.2.4 Research Design

This study used a quantitative research approach.

### 3.2.5 Sampling Techniques and Sample Size

The sampling was done using the simple random method from the data provided by the hospital. The sample size was thirty in total, twenty (20) head and neck cases and ten (10) prostate cases.

### 3.2.6 Acquisition of Images

This study was retrospective; the images used were that of patients who had undergone full treatment. The MV images and kV images used for the study were acquired from the Export option found under the DICOM in Quicklinks in the ARIA treatment planning system at KATH. The image pairs were anonymised and exported in a DICOM format and transferred to a local computer. A total of twenty prostate cases and ten head and neck cases were used.

### 3.2.7 Running of CORRO Algorithm

In this study, the combinatorial rigid registration optimisation (CORRO) landmark point algorithm was used to exemplify a technique for determining the optimal alignment for clinical image sets. The kV and MV image sets (Anterior-Posterior view and Lateral view) were loaded into the assisted expert manual point selection algorithm graphic user interface to select landmark points. Given the image quality of the MV images, corners and angles and pointed anatomy were the regions of focus. The landmark points were used to calculate rigid registration between the kV and MV, and the output translation was applied to the MV image to match the DRR.

### 3.2.8 Computing Results

The output translation from running CORRO gives translations in Tx, Ty, Tz in pixel, but since the images used were 2D planes, the Tx and Ty values were the only outputs considered. These values were then multiplied by the ratio of the image spacing of the image pairs (MV and kV images). The ratio was found because the image spacing for the kV was found to be 0.977 millimetres (mm), while that of the MV was found to be 0.392 millimetres. Based on the viewpoints of the Anterior-Posterior and Lateral views, there were two tx values computed, so the average of the two values was found and recorded. The 2D anterior-posterior viewpoint provides us with an x and z plane, while the lateral viewpoint provides us with the y and x plane. The unit of the standard / clinical values we were comparing to were in centimetres (cm); hence our values had to be converted too.

### 3.2.9 Calculating the Shifts

The results were obtained after loading the image pairs to run an analysis on each image pair by picking corner points on the image pairs for Anterior-Posterior and Lateral views simultaneously. This analysis was done to compare the outcome with that which was done clinically. The tx and ty values gotten after running the registration in the in-house MATLAB algorithm were pixel values. The values were then multiplied by the ratio of the MV and kV image spacing since they did not have the same values. The ratio between MV and kV Image Spacing was achieved by equation (1):

$$\text{The ratio between MV and kV Image Spacing} = \frac{MV\ Image\ Spacing}{kV\ Image\ Spacing} \quad (1)$$

The values were changed to centimetres because the standard (clinical shifts) are in centimetres.

To convert the pixel values to shifts in centimetres using equations (2) and (3):

$$\text{Tx (cm)} = \frac{\text{tx (pixel)} \times \textbf{Ratio}}{\textbf{10}} \quad (2)$$

$$\text{Ty (cm)} = \frac{\text{tx (pixel)} \times \textbf{Ratio}}{\textbf{10}} \quad (3)$$

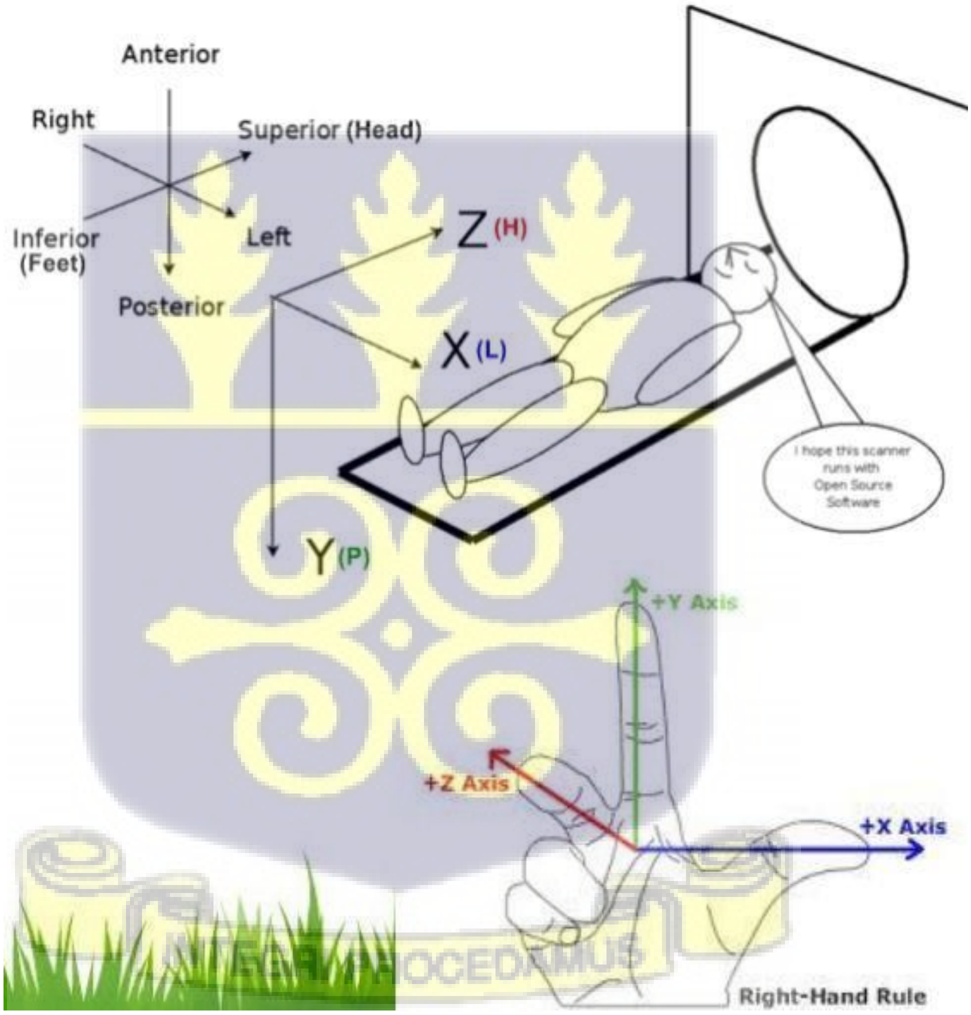


Source: http://mrl.cs.uh.edu/FMI_Fall_2013.html

Figure 7: DICOM Geometry Information

Based on Fig 7 in the information provided, the 2D plane images for the anterior-posterior plane and the 2D lateral plane were translated to provide us with the x, y and z values. For the Anterior-Posterior view, as stated before, the x and z values were gotten, and for the lateral view, x and y values were gotten. The two x values were added and divided by 2 to find the

$$x = \frac{x_{AP} + x_{LAT}}{2} \quad (4)$$

After these values were obtained, they were compared to that of the shifts applied to the Lateral (x), longitudinal (y), and vertical (z) shifts gotten from the treatment room coordinate system. The root mean square of the shifts, that is, that of the ones gotten from the CORRO algorithm and that of the Clinical standard, were found for each case. This was done by using equation 5:

$$\sqrt{(\mathrm{Lat}_{\mathrm{CORRO}} - \mathrm{Lat}_{\mathrm{CLINICAL}})^2 + (\mathrm{Lng}_{\mathrm{CORRO}} - \mathrm{Lng}_{\mathrm{CLINICAL}})^2 + (\mathrm{Vert}_{\mathrm{CORRO}} - \mathrm{Vert}_{\mathrm{CLINICAL}})^2}$$

(5)

# CHAPTER FOUR

## RESULTS AND DISCUSSION

### 4.1 INTRODUCTION

This chapter summarises the study's findings and discusses them. The CORRO algorithm was used to run the image pairs, and the registration provided shifts that were compared to that done clinically. To assist in determining the setup's level of accuracy, the root mean square deviation was calculated.

### 4.2 CALCULATING THE SHIFTS

The results in Tables 1 and 2 are obtained after loading the image pairs and running an analysis on each pair by simultaneously picking corner points, angles, and points on pointed bony landmarks for Anterior-Posterior and Lateral views. Table 3 indicates the shifts calculated from the CORRO algorithm, shifts from the Eclipse Treatment Planning System and the Calculated Root Mean Square Deviation for all prostate cases. The ratio between MV and kV Image Spacing was calculated to be 0.401 mm.

Table 1: A Summation of the CORRO Registration in pixels and millimetres for the 2D Image Pairs for all Prostate Cases.

| Study ID for Prostate Cases | tx (pixel) | ty (pixel) | DRR Image Spacing | MV Image Spacing | Ratio {MV\DRR} | Tx(mm) | Ty(mm) |
|---|---|---|---|---|---|---|---|
| **MS001 (ant)** | -6.561 | -1.635 | 0.977 | 0.392 | 0.401 | -2.633 | -0.656 |
| **MS001 (lat)** | 36.720 | 4.64E+02 | 0.977 | 0.392 | 0.401 | 14.740 | 186.306 |
| **MS002 (ant)** | 16.521 | -8.778 | 0.977 | 0.392 | 0.401 | 6.631 | -3.524 |
| **MS002 (lat)** | -45.023 | 3.95E+02 | 0.977 | 0.392 | 0.401 | -18.072 | 158.553 |
| **MS003 (ant)** | 48.685 | 2.10E+02 | 0.977 | 0.392 | 0.401 | 19.542 | 84.390 |
| **MS003 (lat)** | 73.713 | 1.76E+02 | 0.977 | 0.392 | 0.401 | 29.589 | 70.571 |
| **MS004 (ant)** | 13.893 | -86.521 | 0.977 | 0.392 | 0.401 | 5.577 | -34.730 |
| **MS004 (lat)** | 73.379 | -72.460 | 0.977 | 0.392 | 0.401 | 29.455 | -29.086 |
| **MS005 (ant)** | -20.810 | 28.731 | 0.977 | 0.392 | 0.401 | -8.353 | 11.533 |
| **MS005 (lat)** | 61.944 | -1.15E+02 | 0.977 | 0.392 | 0.401 | 24.865 | -45.971 |
| **MS006(ant)** | -18.318 | -21.709 | 0.977 | 0.392 | 0.401 | -7.353 | -8.714 |
| **MS006 (lat)** | -32.702 | -10.604 | 0.977 | 0.392 | 0.401 | -13.127 | -4.257 |
| **MS007 (ant)** | -12.585 | 10.456 | 0.977 | 0.392 | 0.401 | -5.052 | 4.197 |
| **MS007 (lat)** | -15.0426 | 13.665 | 0.977 | 0.392 | 0.401 | -6.038 | 5.485 |

| Study ID for Prostate Cases | tx (pixel) | ty (pixel) | DRR Image Spacing | MV Image Spacing | Ratio {MV\DRR} | Tx(mm) | Ty(mm) |
|---|---|---|---|---|---|---|---|
| **MS008 (ant)** | -45.215 | 1.21E+02 | 0.977 | 0.392 | 0.401 | -18.150 | 48.572 |
| **MS008 (lat)** | -65.014 | -72.265 | 0.977 | 0.392 | 0.401 | -26.097 | -29.008 |
| **MS009 (ant)** | 8.283 | -7.742 | 0.977 | 0.392 | 0.401 | 3.325 | -3.108 |
| **MS009 (lat)** | -44.778 | 49.521 | 0.977 | 0.392 | 0.401 | -17.974 | 19.878 |
| **MS012 (ant)** | -12.579 | 33.214 | 0.977 | 0.392 | 0.401 | -5.049 | 13.332 |
| **MS012 (lat)** | 11.726 | 24.633 | 0.977 | 0.392 | 0.401 | 4.707 | 9.888 |
| **MS014 (ant)** | 67.704 | -1.433 | 0.977 | 0.392 | 0.401 | 27.177 | -0.575 |
| **MS014 (lat)** | -45.180 | 27.001 | 0.977 | 0.392 | 0.401 | -18.136 | 10.839 |
| **MS015 (ant)** | -22.737 | 1.05E+02 | 0.977 | 0.392 | 0.401 | -9.127 | 42.048 |
| **MS015 (lat)** | 21.688 | -2.12E+01 | 0.977 | 0.392 | 0.401 | 8.706 | -8.512 |
| **MS016 (ant)** | 6.497 | -37.447 | 0.977 | 0.392 | 0.401 | 2.608 | -15.032 |
| **MS016 (lat)** | -1.23E+02 | 81.843 | 0.977 | 0.392 | 0.401 | -49.453 | 32.852 |
| **MS018 (ant)** | 16.708 | 1.15E+02 | 0.977 | 0.392 | 0.401 | 6.707 | 46.011 |
| **MS018 (lat)** | 20.872 | 1.31E+02 | 0.977 | 0.392 | 0.401 | 8.378 | 52.467 |

| Study ID for Prostate Cases | tx (pixel) | ty (pixel) | DRR Image Spacing | MV Image Spacing | Ratio {MV\DRR} | Tx(mm) | Ty(mm) |
|---|---|---|---|---|---|---|---|
| **MS019 (ant)** | -3.043 | -14.768 | 0.977 | 0.392 | 0.401 | -1.222 | -5.928 |
| **MS019 (lat)** | -1.41E+00 | -1.08E+01 | 0.977 | 0.392 | 0.401 | -0.566 | -4.325 |
| **MS020 (ant)** | -20.195 | -55.841 | 0.977 | 0.392 | 0.401 | -8.107 | -22.415 |
| **MS020 (lat)** | -67.356 | -82.884 | 0.977 | 0.392 | 0.401 | -27.037 | -33.270 |
| **MS021 (ant)** | -55.813 | 1.26E+02 | 0.977 | 0.392 | 0.401 | -22.404 | 50.485 |
| **MS021 (lat)** | 42.977 | 1.16E+02 | 0.977 | 0.392 | 0.401 | 17.251 | 46.747 |
| **MS026 (ant)** | -1.284 | -0.190 | 0.977 | 0.392 | 0.401 | -0.516 | -0.076 |
| **MS026 (lat)** | 21.673 | -4.909 | 0.977 | 0.392 | 0.401 | 8.700 | -1.970 |
| **MS027 (ant)** | 42.500 | -84.216 | 0.977 | 0.392 | 0.401 | 17.060 | -33.805 |
| **MS027 (lat)** | 58.639 | -65.672 | 0.977 | 0.392 | 0.401 | 23.538 | -26.361 |
| **MS028 (ant)** | -23.264 | 42.129 | 0.977 | 0.392 | 0.401 | -9.338 | 16.911 |
| **MS028 (lat)** | 6.88E+00 | -2.42E+01 | 0.977 | 0.392 | 0.401 | 2.762 | -9.730 |

Table 2: A Summation of the CORRO Registration in pixels and millimetres for the 2D Image Pairs for all Head and Neck Cases.

| Study ID for Head and Neck Cases | tx (pixel) | ty (pixel) | DRR Image Spacing | MV Image Spacing | Ratio {MV\DRR} | Tx(mm) | Ty(mm) |
|---|---|---|---|---|---|---|---|
| **HMS010 (APt)** | 31.430 | 6.089 | 0.977 | 0.392 | 0.401 | 12.616 | 2.444 |
| **HMS010 (lat)** | -2.68E+02 | -2.09E+02 | 0.977 | 0.392 | 0.401 | -107.432 | -83.789 |
| **HMS011 (AP)** | -6.990 | 25.008 | 0.977 | 0.392 | 0.401 | -2.806 | 10.038 |
| **HMS011 (lat)** | 41.655 | -67.892 | 0.977 | 0.392 | 0.401 | 16.721 | -27.252 |
| **HMS017 (AP)** | -33.941 | 34.459 | 0.977 | 0.392 | 0.401 | -13.624 | 13.832 |
| **HMS017 (lat)** | 4.462 | -9.652 | 0.977 | 0.392 | 0.401 | 1.791 | -3.875 |
| **HMS022 (AP)** | -49.905 | 1.81E+02 | 0.977 | 0.392 | 0.401 | -20.032 | 72.713 |
| **HMS022 (lat)** | -26.603 | 81.498 | 0.977 | 0.392 | 0.401 | -10.679 | 32.714 |
| **HMS023(AP)** | 24.547 | 23.193 | 0.977 | 0.392 | 0.401 | 9.853 | 9.310 |
| **HMS023 (lat)** | -28.277 | -37.597 | 0.977 | 0.392 | 0.401 | -11.351 | -15.092 |
| **HMS025 (AP)** | -17.211 | 2.80E+02 | 0.977 | 0.392 | 0.401 | -6.909 | 112.398 |
| **HMS025 (lat)** | 46.703 | 43.902 | 0.977 | 0.392 | 0.401 | 18.747 | 17.623 |

| Study ID for Head and Neck Cases | tx (pixel) | ty (pixel) | DRR Image Spacing | MV Image Spacing | Ratio {MV\DRR} | Tx(mm) | Ty(mm) |
|---|---|---|---|---|---|---|---|
| **HMS047 (AP)** | -19.458 | 1.33E+02 | 0.977 | 0.392 | 0.401 | -7.811 | 53.441 |
| **HMS047 (lat)** | 29.527 | 7.847 | 0.977 | 0.392 | 0.401 | 11.853 | 3.150 |
| **HMS048 (ant)** | -8.888 | 20.221 | 0.977 | 0.392 | 0.401 | -3.568 | 8.117 |
| **HMS048 (lat)** | -11.501 | -4.673 | 0.977 | 0.392 | 0.401 | -4.617 | -1.876 |
| **HMS049 (ant)** | -10.655 | 47.697 | 0.977 | 0.392 | 0.401 | -4.277 | 19.146 |
| **HMS049 (lat)** | -16.629 | -72.944 | 0.977 | 0.392 | 0.401 | -6.675 | -29.280 |
| **HMS050 (ant)** | -40.500 | 54.735 | 0.977 | 0.392 | 0.401 | -16.257 | 21.971 |
| **HMS050 (lat)** | -12.665 | 13.823 | 0.977 | 0.392 | 0.401 | -5.084 | 5.549 |

Table 3: A table showing the shifts calculated from the CORRO algorithm, shifts from the Eclipse Treatment Planning System and the Calculated Root Mean Square Deviation for all Prostate cases.

| PROSTATE | | | | | | | |
|---|---|---|---|---|---|---|---|
| **Study ID** | **Lat_CORRO (cm)** | **Lng_CORRO (cm)** | **Vrt_CORRO (cm)** | **Lat_clinical (cm)** | **Lng_Clinical (cm)** | **Vrt_Clinical (cm)** | **Root Mean Square** $\sqrt{(x_{Corro}-x_{Clincal})2+(y_{Corro}-y_{Clincal})2+(z_{Corro}-z_{Clincal})2)}$ |
| **MS001** | 0.6 | 18.6 | -0.1 | 0.0 | 0.0 | -0.6 | 18.616 |
| **MS002** | -0.6 | 15.9 | -0.4 | -0.8 | 0.4 | -1.3 | 15.527 |
| **MS003** | 2.5 | 7.1 | 8.4 | 1.6 | -3.0 | 0.8 | 12.672 |
| **MS004** | 1.8 | -2.9 | -3.5 | 0.1 | 1.6 | 1.7 | 7.084 |
| **MS005** | 0.8 | -4.6 | 1.2 | 1.1 | 0.2 | -0.2 | 5.009 |
| **MS006** | -1.0 | -0.4 | -0.9 | -0.4 | 0.1 | -0.9 | 0.781 |
| **MS007** | -0.6 | 0.5 | 0.4 | 0.6 | -4.1 | -17 | 18.038 |
| **MS008** | -2.2 | -2.9 | 4.9 | 0.0 | -0.3 | -3.3 | 8.879 |
| **MS009** | -0.7 | 2.0 | -0.3 | 0.0 | -0.4 | 0.2 | 2.550 |

| Study ID | Lat_CORRO (cm) | Lng_CORRO (cm) | Vrt_CORRO (cm) | Lat_clinical (cm) | Lng_Clinical (cm) | Vrt_Clinical (cm) | Root Mean Square $\sqrt{(x_{Corro}-x_{Clincal})2+(y_{Corro}-y_{Clincal})2+(z_{Corro}-z_{Clincal})2)}$ |
|---|---|---|---|---|---|---|---|
| **MS012** | 0.0 | 1.0 | 1.3 | -1.3 | -2.3 | 0.0 | 3.778 |
| **MS014** | 0.5 | 1.1 | -0.1 | 0.3 | 0.7 | 0.0 | 0.458 |
| **MS015** | 0.0 | -0.9 | 4.2 | -0.7 | -0.7 | -0.8 | 5.053 |
| **MS016** | -2.3 | 3.3 | -1.5 | 0.7 | 1.6 | 1.4 | 4.506 |
| **MS018** | 0.8 | 5.2 | 4.6 | -1.9 | -3.2 | 0.0 | 9.950 |
| **MS019** | -0.1 | -0.4 | -0.6 | 1.1 | 1.8 | 2.3 | 3.833 |
| **MS020** | -1.8 | -3.3 | -2.2 | -0.7 | 2.6 | -0.2 | 6.326 |
| **MS021** | -0.3 | 4.7 | 5.0 | -1.2 | 1.0 | 0.2 | 6.127 |
| **MS026** | 0.4 | -0.2 | -0.0 | 1.2 | 0.8 | 0.3 | 1.315 |
| **MS027** | 2.0 | -2.6 | -3.4 | -1.1 | 0.6 | -0.5 | 5.316 |
| **MS028** | -0.3 | -1.0 | 1.7 | 0.3 | 0.5 | -0.2 | 2.494 |

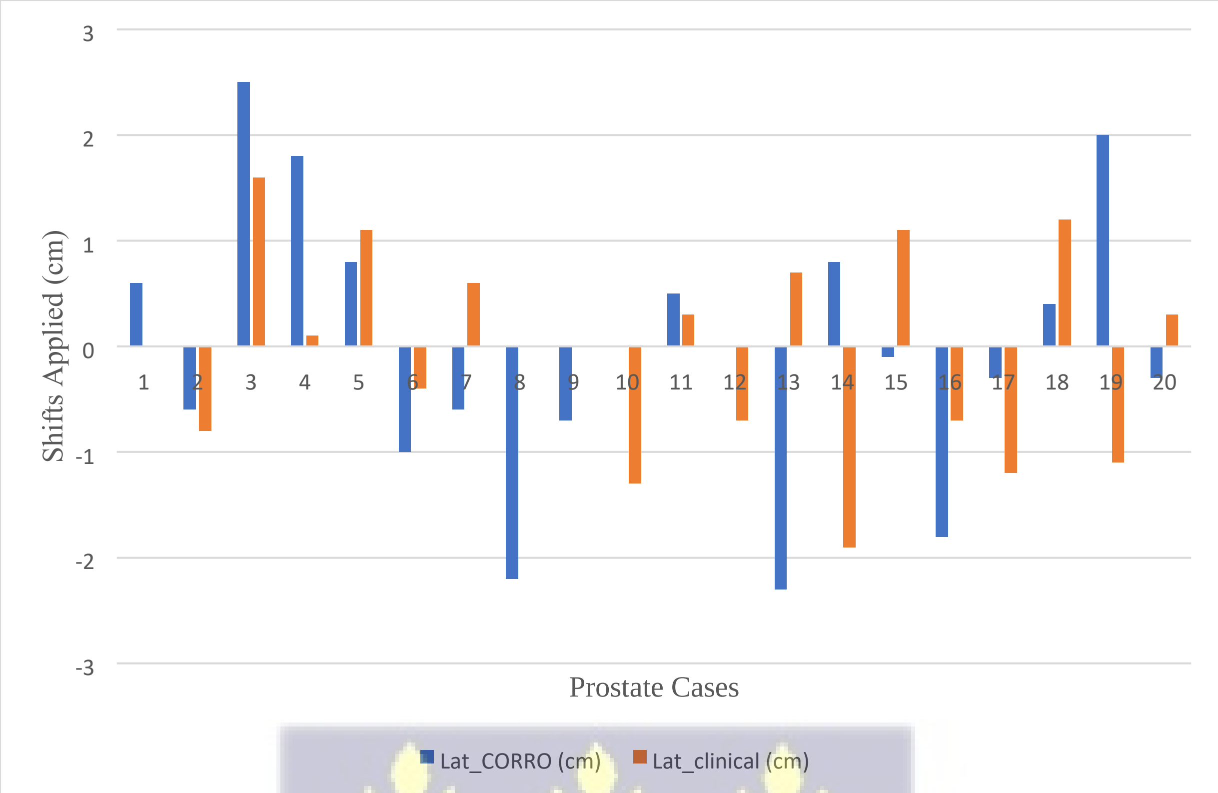


Figure 8: Graphical View of the Variation in Shifts in the Lateral Direction for Prostate Cases.

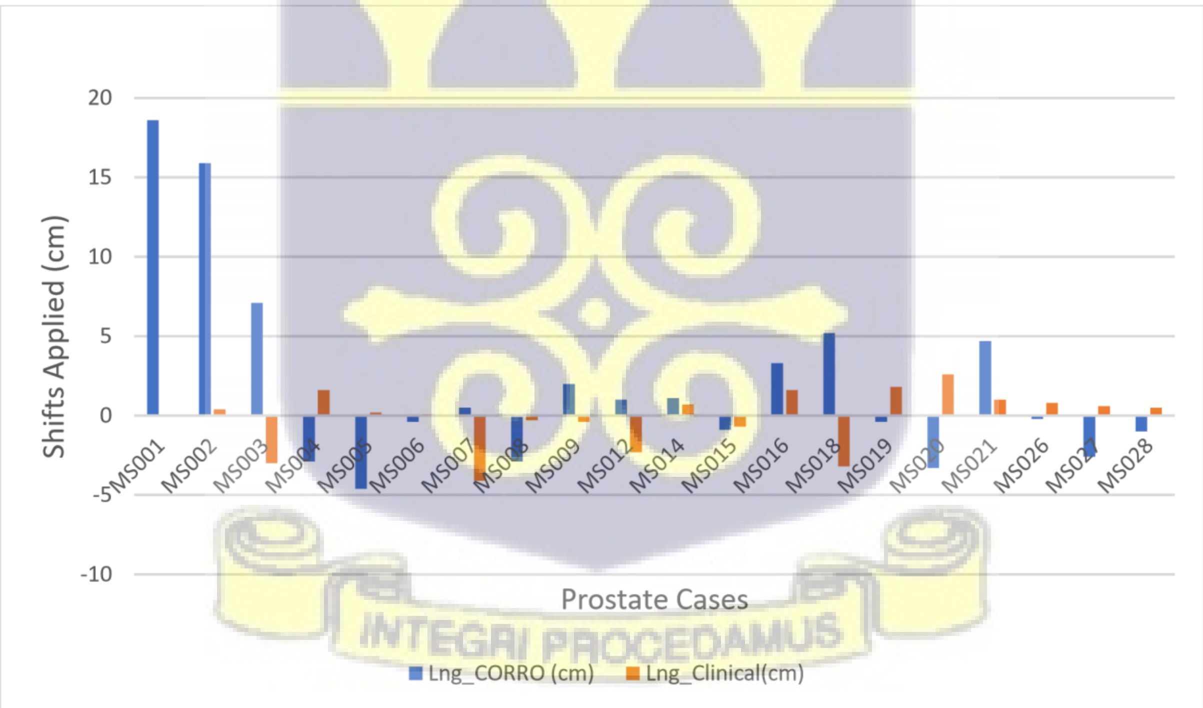


Figure 9: Graphical View of the Variation in Shifts in the Longitudinal Direction for Prostate Cases.

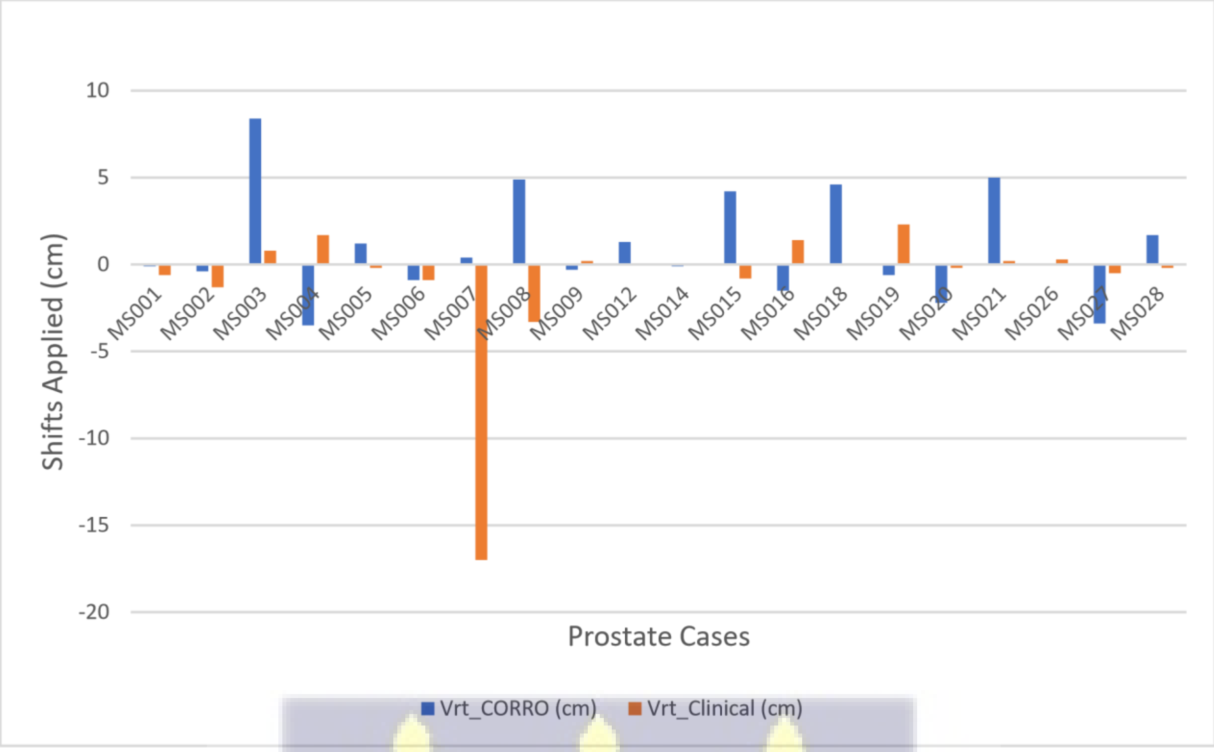


Figure 10: Graphical View of the Variation in Shifts in the Vertical Direction for Prostate Cases

Figures 8 to 10 shows a graphical view of the deviations occurring between the scaled CORRO output registration and the Clinal shift. The figures show large differences hence showing that there is a lack of accuracy when it comes to patient setup reproducibility.

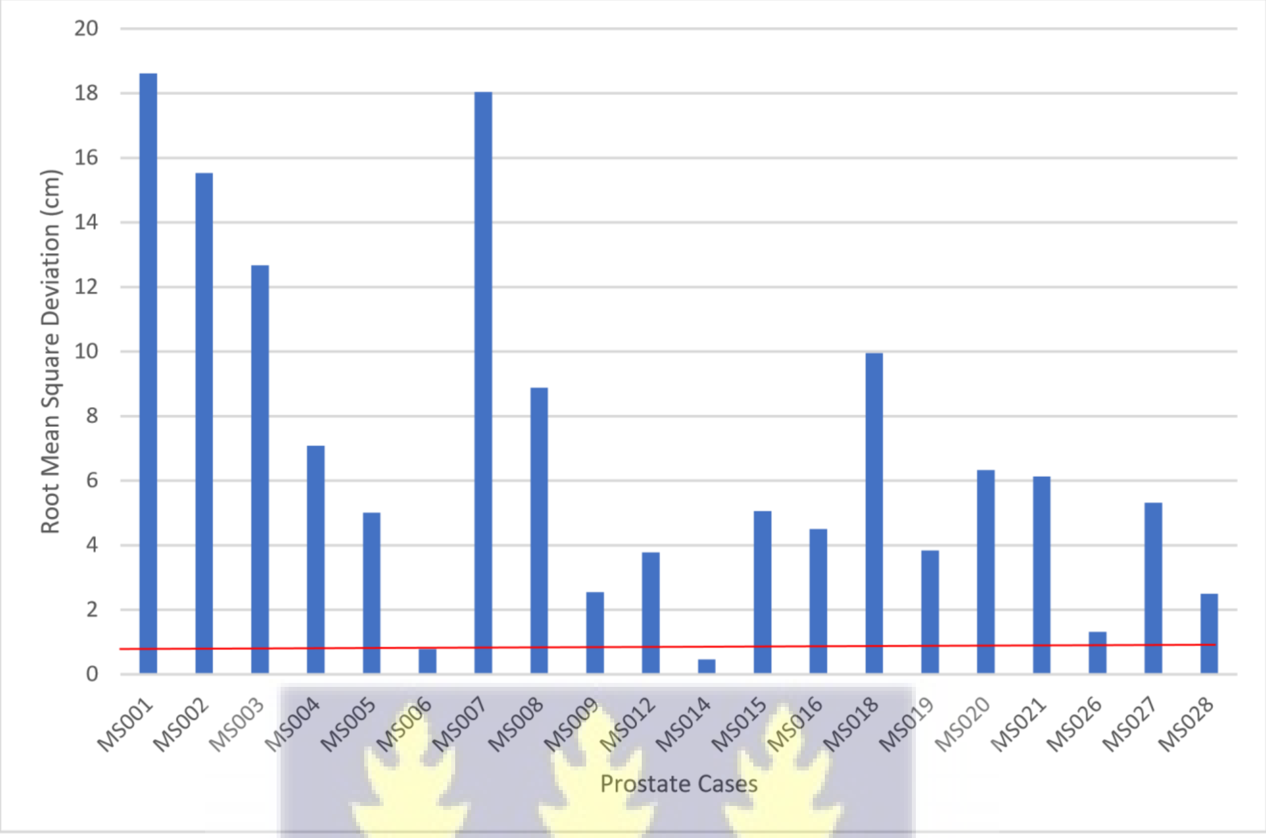


Figure 11: Graphical View of the Deviations Occurring in the Setup for Prostate cases.

Figure 11 is a graphical representation of the root mean square deviation that was calculated to find the deviation occurring between the two registrations. It was found that the root mean square deviations occurring in the shifts between that of the CORRO algorithm and that of the Clinical standard for the Prostate cases was found to be in the range of 0.46 cm – 18.62 cm. The range buttresses the lack of patient setup accuracy in the facility. The cases whose bar are below the red line in the graph are the cases that passed the facility's accuracy mark.

Table 4: A table showing the shifts calculated from CORRO, Eclipse Treatment Planning System and the Root Mean Square Deviation for all Head and Neck Cases.

| HEAD AND NECK | | | | | | | |
|---|---|---|---|---|---|---|---|
| | **Lat_CORRO (cm)** | **Lng_CORRO (cm)** | **Vrt_CORRO (cm)** | **Lat_clinical (cm)** | **Lng_Clinical (cm)** | **Vrt_Clinical (cm)** | **Root Mean Square** $\sqrt{(x_{Corro}-x_{Clincal})^2+(y_{Corro}-y_{Clincal})^2+(z_{Corro}-z_{Clincal})^2}$ |
| **HMS010** | -4.7 | -8.4 | 0.2 | -0.2 | 0.3 | 0.4 | 9.7969 |
| **HMS011** | 0.7 | -2.7 | 1.0 | -0.2 | 0.4 | -0.2 | 3.4438 |
| **HMS017** | -0.6 | -0.4 | 1.4 | 0.0 | 0.0 | 0.0 | 1.5748 |
| **HMS022** | -1.6 | 3.3 | 7.3 | 0.0 | 0.0 | 2.3 | 6.2008 |
| **HMS023** | -0.1 | -1.5 | 0.9 | 0.0 | 0.0 | 0.0 | 1.7521 |
| **HMS025** | 0.6 | 1.8 | 11.2 | -0.4 | 0.2 | -0.2 | 11.5551 |
| **HMS047** | 0.2 | 0.3 | 5.3 | 0.0 | 0.6 | -0.1 | 5.4120 |
| **HMS048** | -0.5 | -0.2 | 0.8 | 1.0 | -0.2 | 0.1 | 1.6553 |
| **HMS049** | -0.6 | -2.9 | 1.9 | 0.0 | -0.4 | 0.6 | 2.8810 |
| **HMS050** | -1.1 | 0.6 | 2.2 | -2.9 | -3.6 | -1.8 | 6.0729 |

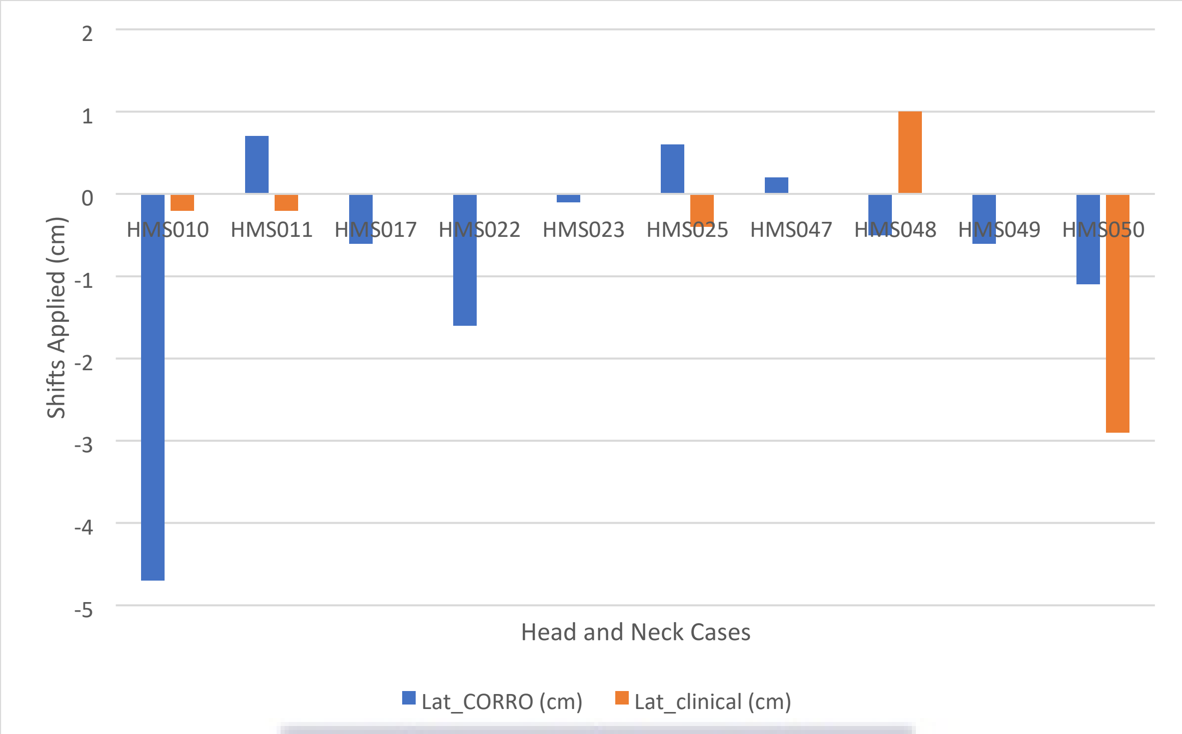


Figure 12: Graphical View of the Variation in Shifts in the Lateral Direction for Head and Neck Cases.

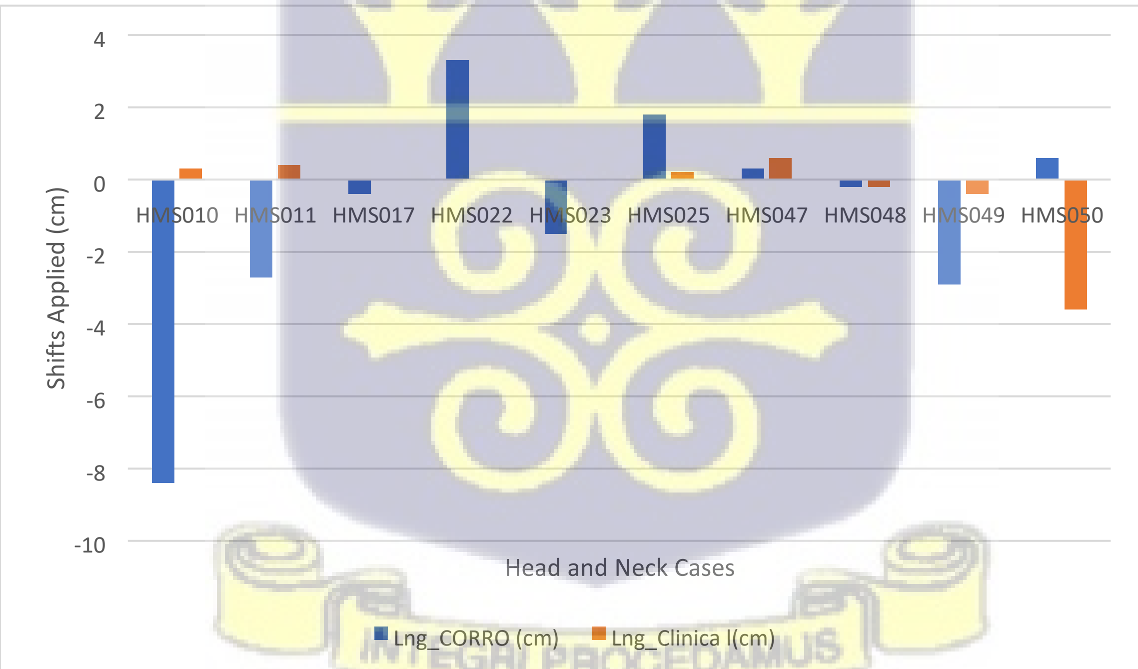


Figure 13: A Graphical View of the Variation in Shifts in the Longitudinal Direction for Head and Neck Cases.

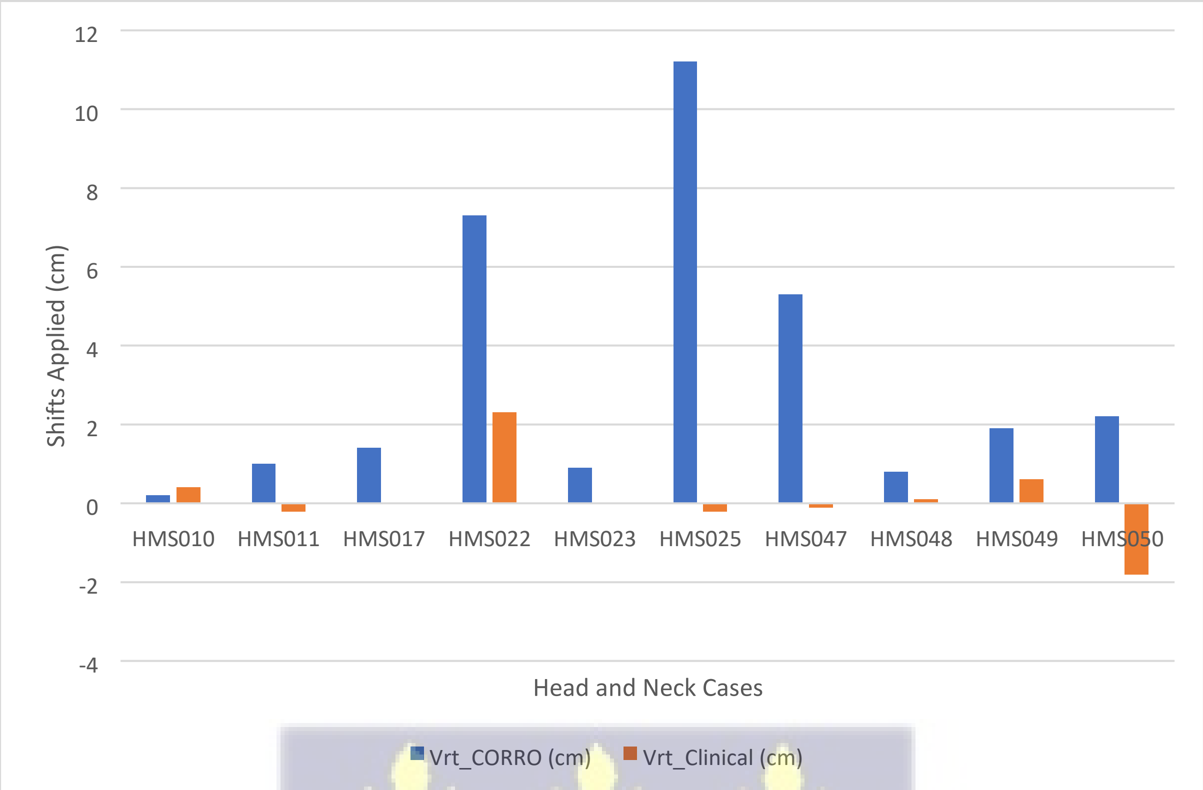


Figure 14: A Graphical View of the Variation in Shifts in the Vertical Direction for Head and Neck Cases.

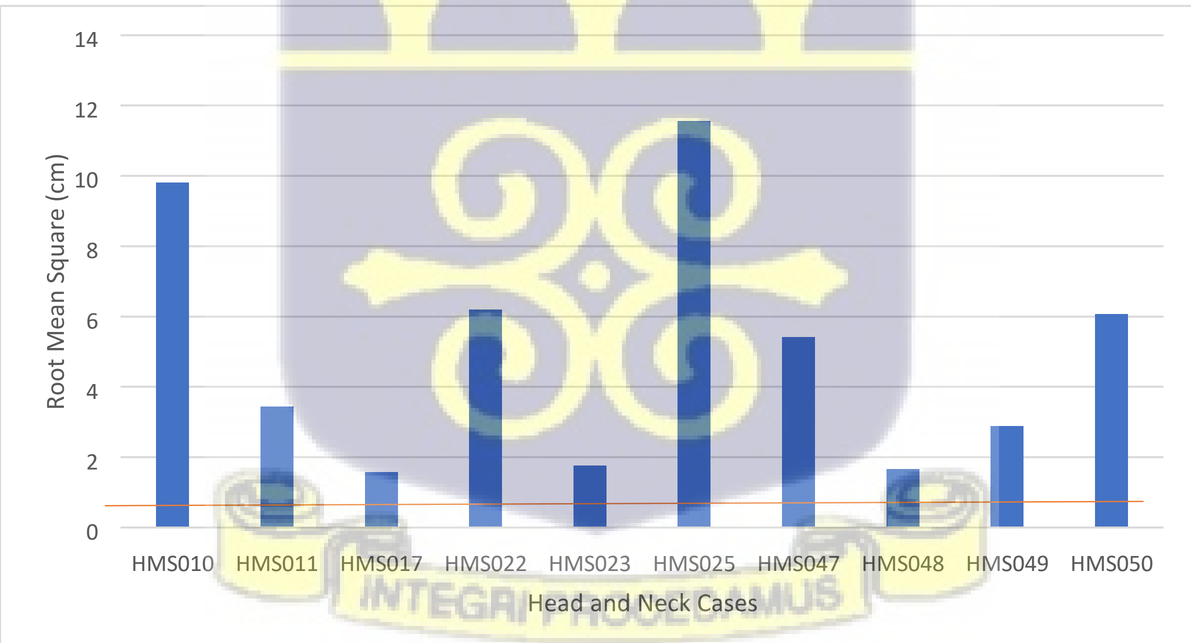


Figure 15: A Graphical View of the Deviations Occurring in the Setup for Head and Neck cases.

Figures 12 to 14 represents the differences between the CORRO and Clinical Lateral, Longitudinal and Vertical shifts respectively. The graphs show large variations between the two registration and these were because of the poor patient positioning, as could be seen in the offline review images. These were of much concern because they indicated the lack of precision and accuracy in the setup, and hence this led to the toxicity of healthy tissues, which goes against the aim of radiotherapy.

Figure 15 represents the graphical view of the root mean square deviation calculated for the CORRO and Clinical shifts for each head and neck case. The root mean square deviations occurring in the shifts between that of the CORRO algorithm and that of the Clinical standard of the Head and Neck was found to be between 1.57 cm – 11.56 cm. This represents the systematic error for both cases. The deviations occurring shows that there are large shift differences between that gotten from CORRO, which is being used for the quality assurance of the setup and that of which is done clinically. This proves that there is a gap that needs to be filled when it comes to the patient setup at the study location. The bars below the red line in figure 15 represents the cases that passed the accuracy standard of the facility, all others failed.

Limitations faced in this study were:

1. Resizing of the kV image: The kV image was 512×512 in size while the MV image was 768×1024 in size when exported. The MV image displayed the region of interest for treatment hence the kV image had to be resized to display the same region and also to aid in making the mutual point picking easier since the two images will have the same resolution.
2. Older versions of MATLAB , that is, R2013b and below did not support the algorithms used in the work.

# CHAPTER FIVE

## CONCLUSIONS AND RECOMMENDATION

### 5.1 CONCLUSIONS

Quality assurance of the patient setup process at the KATH has been performed using the CORRO algorithm to analyse twenty prostate cases and ten head and neck cases. The results showed discrepancies from what was expected. There are large deviations between the clinical and CORRO algorithm in longitudinal, lateral, and vertical. The results computed showed poor setup accuracy.

The poor accuracy in the setup can be a result of the patients getting their simulation CT from outside institutions, and this can be a contributing factor since normally, Radiotherapists are supposed to be present during patient simulation, or notes are placed in the record verify system, which acts as a guide for the patient setup.

### 5.2 RECOMMENDATIONS

It is well documented that patient setup plays a very vital role in delivering the prescribed dose to the target. Any misalignment will be detrimental to the patient. For radiotherapy centres in the process of transitioning from Co-60 to modern linear accelerators without kV imaging capabilities to guide in the patient set up process, it is recommended to the study facility and all radiation treatment facilities to do periodic quality assurance on the patient setup process and correct any discrepancies that may show up in the clinical workflow.

It is also recommended to the facility that the Radiotherapist need to be educated and trained on how to properly set up patients.

# REFERENCES

Aanér, E., Petri, A., Sorcini, B., & Mäslund, I. (2005). 534 Patient setup verification with online MV-portal imaging and displacement adjustment by the technician. *Radiotherapy and Oncology*, (76), S227.

Boda-Heggemann J, Lohr F, Wenz F, Flentje M & Guckenberger M. (2011). kV cone-beam CT- based IGRT. Strahlentherapie Onkologie Journal; 187:284–291.

Chai, W., Zhao, Q., Song, H., Cheng, C., Tian, G., & Jiang, T. A. (2019). Treatment response and preliminary efficacy of hepatic tumour laser ablation under the guidance of percutaneous and endoscopic ultrasonography. *World journal of surgical oncology*, *17*(1), 1-8.

Clippe S, Sarrut D, Malet C, Miguet S, Ginestet C, Carrie C. Patient setup error measurement using 3D intensity-based image registration techniques. Int J Radiat Oncol Biol Phys. 2003;56:259–265

Dorgham, O., Ryalat, M. H., & Naser, M. A. (2020). Automatic body segmentation for accelerated rendering of digitally reconstructed radiograph images. *Informatics in Medicine Unlocked*, *20*, 100375.

Ébastien Clippe, S., Sarrut, D., Malet, C., Miguet, S., Ginestet, C., & Carrie, C. (2003). Patient setup error measurement using 3D intensity-based image registration techniques. *International Journal of Radiation Oncology* Biology* Physics*, *56*(1), 259-265.

Eclipse™ Treatment Planning Software from Varian Medical Systems Named a "Category Leader” in the 2014 “Best in KLAS: Software and Services Report” https://www.varian.com/de/node/7723

Govindaraj, Ramesh; A.A.D. Obuobi; N.K.A. Enyimayew; P. Antwi; S. Ofosu-Amaah (August 1996). "Hospital Autonomy (GEE) in Ghana: The Experience of Korle Bu and Komfo Anokye Teaching Hospitals" (PDF). Data for Decision Making Project. School of

Public Health, University of Ghana and Harvard School of Public Health. Retrieved 8th June 2022.

Goyal, S., & Kataria, T. (2014). Image guidance in radiation therapy: techniques and applications. *Radiology research and practice, 2014*.

Graham, R. N., Perriss, R. W., & Scarsbrook, A. F. (2005). DICOM demystified: a review of digital file formats and their use in radiological practice. *Clinical radiology*, *60*(11), 11331140.

Hashimoto, S., Shirato, H., Nishioka, T., Kagei, K., Shimizu, S., Fujita, K., ... & Miyasaka, K. (2001). Remote verification in radiotherapy using digitally reconstructed radiography (DRR) and portal images: a pilot study. *International Journal of Radiation Oncology* Biology* Physics*, *50*(2), 579-585.

Image-guided radiation therapy (IGRT) - Drugs.com. https://www.drugs.com/mcp/imageguided-radiation-therapy-igrt

J. Chang, G. S. Mageras, C. S. Chui, C. C. Ling, and W. Lutz. (2000). "Relative profile and dose verification of intensity-modulated radiation therapy," Int. J. Radiat. Oncol., Biol., Phys. 47, 231–240

Junmo An. (2013) Fundamentals of Medical Imaging. MATLAB Tutorial II – University of Houston. http://mrl.cs.uh.edu/FMI_Fall_2013.html

Kim, J., Fessler, J. A., Lam, K. L., Balter, J. M., & Ten Haken, R. K. (2001). A feasibility study of mutual information based setup error estimation for radiotherapy. Medical Physics, 28(12), 2507-2517.

Komfo Anokye Teaching Hospital (KATH), 2022. Retrieved from http://www.kathhsp.org/oncology-directorate/, retrieved on 8th June, 2022.

Kron, T. (2008). Reduction of margins in external beam radiotherapy. Journal of Medical Physics/Association of Medical Physicists of India, 33(2), 41.

LINAC (Linear Accelerator). https://www.radiologyinfo.org/en/info/linac

About - Mayo Clinic. https://www.mayoclinic.org/tests-procedures/image-guided-radiationtherapy/about/pac-20385267?p=1

Lei Dong, Arthur L. Boyer.(1995) An image correlation procedure for digitally reconstructed radiographs and electronic portal images. International Journal of Radiation Oncology*Biology*Physics, Volume 33, Issue 5, 1995, Pages 1053-1060, ISSN 0360-3016, https://doi.org/10.1016/0360-3016(95)02082-9.

Li, Yanmin, et al. "The Effects of High-Frequency RTMS over the Left DLPFC on Cognitive Control in Young Healthy Participants." PLoS One, vol. 12, no. 6, Public Library of Science, June 2017, p. e0179430.

LoSasso, T., Chui, C. S., & Ling, C. C. (2001). Comprehensive quality assurance for the delivery of intensity-modulated radiotherapy with a multileaf collimator used in the dynamic mode. *Medical physics*, *28*(11), 2209-2219.

MATLAB Resources, Introduction to MATLAB and MATLAB Scripting, retrieved on !5th December on https://guides.libraries.uc.edu/c.php?g=461109&p=3152738

O'Neill AGM, Jain S, Hounsell AR, O'Sullivan JM. Fiducial marker guided prostate radiotherapy: a review. Br J Radiol. 2016;89:20160296.

Pehlivan, B., Pichenot, C., Castaing, M., Auperin, A., Lefkopoulos, D., Arriagada, R., & Bourhis, J. (2009). Interfractional setup errors evaluation by daily electronic portal imaging of IMRT in head and neck cancer patients. *Acta Oncologica*, *48*(3), 440-445.

Pluim, J. P., Maintz, J. A., & Viergever, M. A. (2003). Mutual-information-based registration of medical images: a survey. *IEEE transactions on medical imaging*, *22*(8), 986-1004.

Poggi, M. M., Gant, D. A., Sewchand, W., & Warlick, W. B. (2003). Marker seed migration in prostate localisation. *International Journal of Radiation Oncology* Biology* Physics*, *56*(5), 1248-1251.

Schoonbeek, A., Monshouwer, R., Hanssens, P., Raaijmakers, E., Nowak, P., Marijnissen, J. P. A., ... & van der Maazen, R. W. M. (2010). Intracranial radiosurgery in the Netherlands. A planning comparison of available systems with regard to physical aspects and workload. *Technology in cancer research & treatment*, *9*(3), 279-289.

Seixas, F. L., Damasceno, J., de Souza, A. S., Saade, D. C. M., & da Silva, M. P. (2007, October). Automatic segmentation of brain structures based on anatomic atlas. In *Seventh International Conference on Intelligent Systems Design and Applications (ISDA 2007)* (pp. 329-334). IEEE.

Shamir RR & Joskowicz L. (2011). Geometrical analysis of registration errors in point-based rigid-body registration using invariants. Medical Image Analysis Journal;15:85–95.

Stabinger, S., Peer, D., Piater, J., & Rodríguez-Sánchez, A. (2021). Evaluating the progress of deep learning for visual relational concepts. *Journal of Vision, 21*(11), 8-8.

Sutherland K, Ishikawa M, Bengua G, Ito YM, Miyamoto Y & Shirato H. (2011). Detection of patient setup errors with a portal image - DRR registration software application. Journal of Applied Clinical Medical Physics; 12:3492.

van der Heide, U. A., Kotte, A. N., Dehnad, H., Hofman, P., Lagenijk, J. J., & van Vulpen, M. (2007). Analysis of fiducial marker-based position verification in the external beam radiotherapy of patients with prostate cancer. *Radiotherapy and oncology*, *82*(1), 38-45.

Verellen D, Ridder MD & Storme GA. (2008). A (short) history of image-guided radiotherapy. Radiotherapy Oncology; 86(1):4-13. doi: 10.1016/j.radonc.2007.11.023

Wong, J., Jaffray, D., & Yin, F. F. The Role of In-Room kV X-Ray Imaging for Patient Setup and Target Localization (TG104).

Woods, R. P., Cherry, S. R., & Mazziotta, J. C. (1992). Rapid automated algorithm for aligning and reslicing PET images. *Journal of computer assisted tomography*, *16*(4), 620-633.

Yorke AA, Solis DJ & Guerrero T. (2020). A feasibility study to estimate optimal rigid-body registration using combinatorial rigid registration optimisation (CORRO). Journal of Applied Clinical Medical Physics;1–9. doi: 10.1002/acm2.12965

(https://www.sciencedirect.com/science/article/pii/0360301695020829)

# APPENDICES

## APPENDIX A: An Image of the MATLAB interface

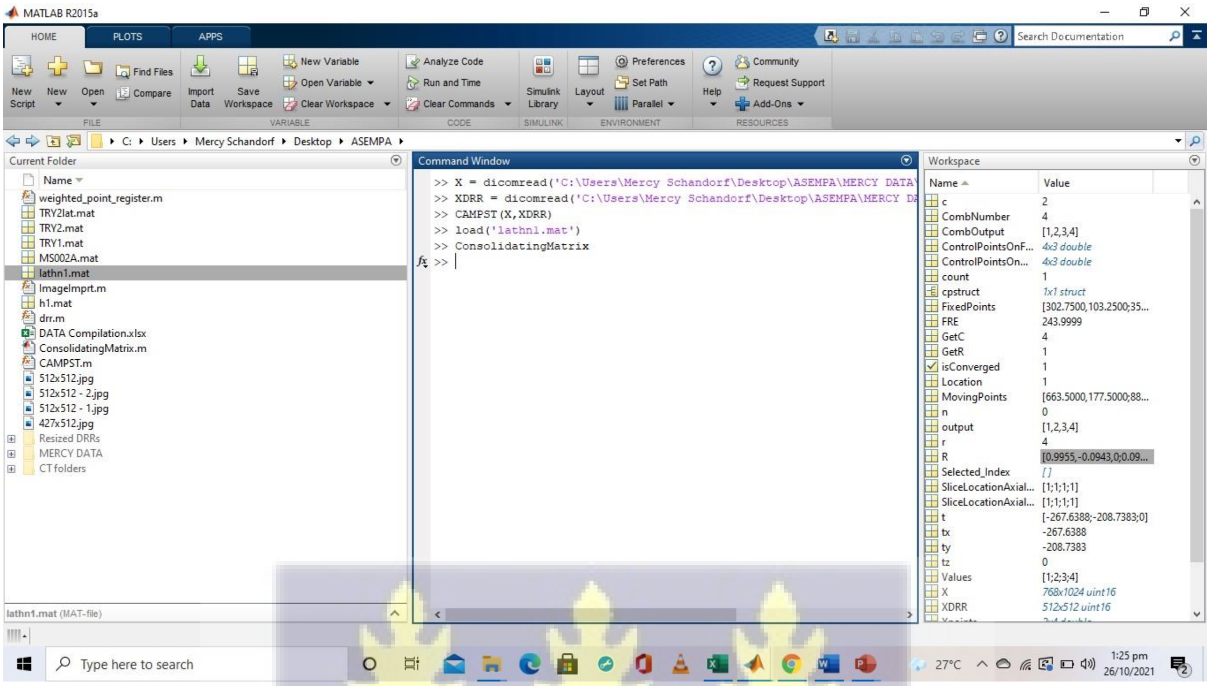


## APPENDIX B: Output of Image Pair loaded in the ASEMPA algorithm

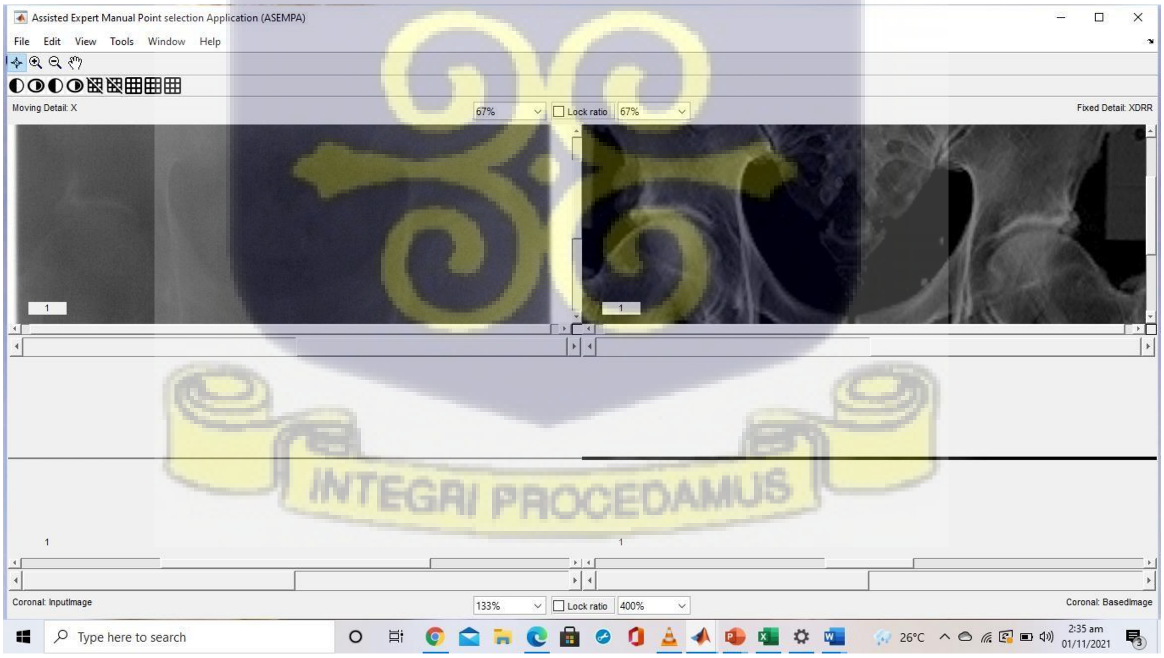

APPENDIX C: Ethical clearance from KATH IRB

**KOMFO ANOKYE**
TEACHING HOSPITAL

P. O. Box 1934
Kumasi - Ghana
**Tel:** +233 - 3200-22301 - 4
**Fax:** +233 - 3220-24654 / 24621
**Website:** www.kathhsp.org

Our Ref. No.:....*KATH IRB/AP/098/21*

Your Ref... No:.......................................

## Komfo Anokye Teaching Hospital Institutional Review Board

14th October 2021

Miss. Mercy Torshie Schandorf
School of Nuclear and Allied Sciences
Medical Physics Department,
University of Ghana,
Legon-Accra

Dear Miss. Schandorf,

**Ethics approval**

| | |
|---|---|
| **Protocol title:** | Quality Assurance of Patient Setup Using MV Portal Imaging and Digitally Reconstructed Radiograph in Radiotherapy Practice. |
| **Study site:** | Oncology Directorate of the Komfo Anokye Teaching Hospital |
| **Sponsor:** | Self-funded |

We write in response to the clarifications and revised documents following review by the Komfo Anokye Teaching Hospital Institutional Review Board (KATH IRB) in respect of the research study referenced above.

We are pleased to inform you that KATH IRB, per your correspondence of 6th September 2021, has given approval for the following study documents:

- *Protocol version 1.1 last updated 30th August 2021*

Approval for the study is in effect until **13th October 2022** and it is the responsibility of the Principal Investigator to maintain the study in good standing at the Komfo Anokye Teaching Hospital. The Board anticipates to be notified of the actual start date of your project.

Prior to the expiration of the study approval, you must submit to the KATH IRB an "Application for Continuing Review" along with provision of "Annual Report" when the study is ongoing, or a "Termination Report" if the research has been completed.

You must hastily report to the KATH IRB should a modification to the research be proposed, and without delay if an unanticipated development occurs before the next required review. Regulations do not permit you to modify conduct of the study in its present form prior to ethics approval; except where urgent action is required to eliminate an apparent immediate hazard to

A Centre of Excellence
Page 1 of 2

a study subject or other person. It is of utmost importance data generated from this study must be used for the intended purposes only.

Thank you.

Sincerely,

Prof. Kwabena Antwi Danso, BSc, MB ChB, FWACS, FGCS, FACOG
Chairman, KATH-IRB

APPENDIX D: Ethical clearance from Ethical Committee of College of Basic Sciences

UNIVERSITY OF GHANA
ETHICS COMMITTEE FOR BASIC AND APPLIED SCIENCES (ECBAS)

*P. O. Box LG 1195, Legon, Accra, Ghana*

Ref. No: ECBAS 053/20-21

8th September, 2021.

Ms. Mercy Torshie Schandorf
Department of Medical Physics
University of Ghana
Legon, Accra

Dear Ms. Schandorf,

**ECBAS 053/20-21: QUALITY ASSURANCE OF PATIENT SETUP USING MV PORTAL IMAGING AND DIGITALLY RECONSTRUCTED RADIOGRAPH IN RADIOTHERAPY PRACTICE**

This is to inform you that the above referenced study has been presented to the Ethics Committee for Basic and Applied Sciences for a full board review and the following actions taken subject to the conditions and explanation provided below:

| | |
|---|---|
| **Expiry Date:** | 19/09/2022 |
| **On Agenda for:** | Initial Submission |
| **Date of Submission:** | 20/06/2021 |
| **ECBAS Action:** | Approved |
| **Reporting:** | Annually |

Please accept my congratulations.

Yours sincerely,

Professor Daniel Bruce Sarpong

ETHICS COMMITTEE FOR BASIC AND APPLIED SCIENCES
APPROVED
13 SEP 2021
UNIVERSITY OF GHANA